

Fig. 6 (continued).

Construction of 2b/JFH-1 based intragenotypic chimeras and transfection

Chimeric HCV constructs of HCV-2b and JFH1 were shown in Figs. 1A and 7A. To construct 2b/JFH1-based intragenotypic chimera, JE31F, the 2b sequence of core through E2 (nt. 342–2541) was fused to the EcoRI-JFH1-5'-untranslated region (UTR) DNA by fusion PCR. The fused 5'UTR-E2 fragment and JFH1-E2-NS3 (nt2541 through 5324) were assembled by fusion PCR and cloned into pGEM-T EASY. The product was digested by EcoRI and AfeI and insert into pJFH1. Plasmids pJE39F, pJEC3F, pJcoreC3F and p2bcore JFH1 were constructed using a similar procedure. Plasmids pJEC3F and pJE39F were joined between NS2 and NS3, and within NS2 at nt. 2867, respectively. Plasmid pJcoreC3F was made by substitution of the core region of 2b/JFH1 with that of JFH1. The plasmid p2bcoreJFH1 was made by substitution of the core region of JFH1 with that of 2b/JFH1.

Cells and cell culture

Huh7.5.1 cells were maintained in Dulbecco's modified minimal essential medium (Sigma, St. Louis, MO) supplemented with 10% fetal calf serum at 37 °C under 5% CO₂.

HCV cell culture system

Full-length HCV expression plasmids were as follows: pJFH1-full (Wakita et al., 2005), pJE31F, pJE39F, pJEC3F, pJcoreC3F, p2bcoreJFH1, and pFL-H77/JFH1, pFL-J6/JFH1 (Lindenbach et al., 2005). These plasmids were linearized at their 3' ends and used as templates for HCV RNA synthesis using the RiboMax Large Scale RNA Production System (Promega, Madison, WI). After DNase I (RQ-1, RNase-free DNase, Promega) treatment, the HCV RNA was purified using ISOGEN (Nippon Gene, Tokyo, Japan). For the RNA transfection, Huh7.5.1 cells were washed twice with PBS, and 5 × 10⁶ cells were suspended in Opti-MEM I (Invitrogen Carlsbad, CA) containing 10 µg of HCV RNA, transferred into a 4 mm electroporation cuvette and finally subjected to an electric pulse (1,050 µF and 270 V) using the Easy Jet system (EquiBio, Middlesex, UK). After electroporation, the cell suspension

was left for 5 min at room temperature and then incubated under normal culture conditions in a cell culture dish.

Quantification of HCV core antigen in culture supernatants

Culture supernatants of HCV RNA transfected Huh7.5.1 cells were collected on the days indicated, passed through a 0.45 µm filter (MILLEX-HA, Millipore, Bedford, MA) and stored at -80 °C. The concentrations of core antigen in the culture supernatants were measured using a chemiluminescence enzyme immunoassay (CLEIA) according to the manufacturer's protocol (Lumipulse Ortho HCV Antigen, Ortho-Clinical Diagnostics, Tokyo, Japan).

Re-infection analyses

Titer-adjusted supernatants (including 0.03 fmol HCV core antigen) from HCV RNA-transfected cells were inoculated onto naïve Huh7.5.1 cells plated on a 6 cm plate at a density of 3 × 10⁵ cells per plate. Forty-eight hours after inoculation, anti-core immunostaining was carried out with mouse anti-HCV core protein monoclonal antibody and the numbers of infected cells were counted. HCV core antigen in culture supernatants was measured at 24 hours, 48 hours, 72 hours and 144 hours after inoculation.

Real-time RT-PCR analysis

For the detection of HCV RNA in culture supernatant, supernatant was passed through a 0.45 µm filter (MILLEX-HA, Millipore, Bedford, MA) and stored at -80 °C until use. Protocol and primers for the realtime RT-PCR analysis of HCV-RNA has been described previously (Sekine-Osajima et al., 2008). For the detection of endogenous mRNAs, total cellular RNA was isolated using ISOGEN (Nippon Gene). Two micrograms of total cellular RNA were used to generate cDNA from each sample using SuperScript II. Expression of mRNA was quantified using the TaqMan Universal PCR Master Mix and the ABI 7500 Real-Time PCR System (Applied Biosystems, Foster City CA). Some primers have been described (Sekine-Osajima et al., 2008). SOCS3; forward, 5'-CAC ATG GCA CAA GCA CAA GAA G-3' and reverse,

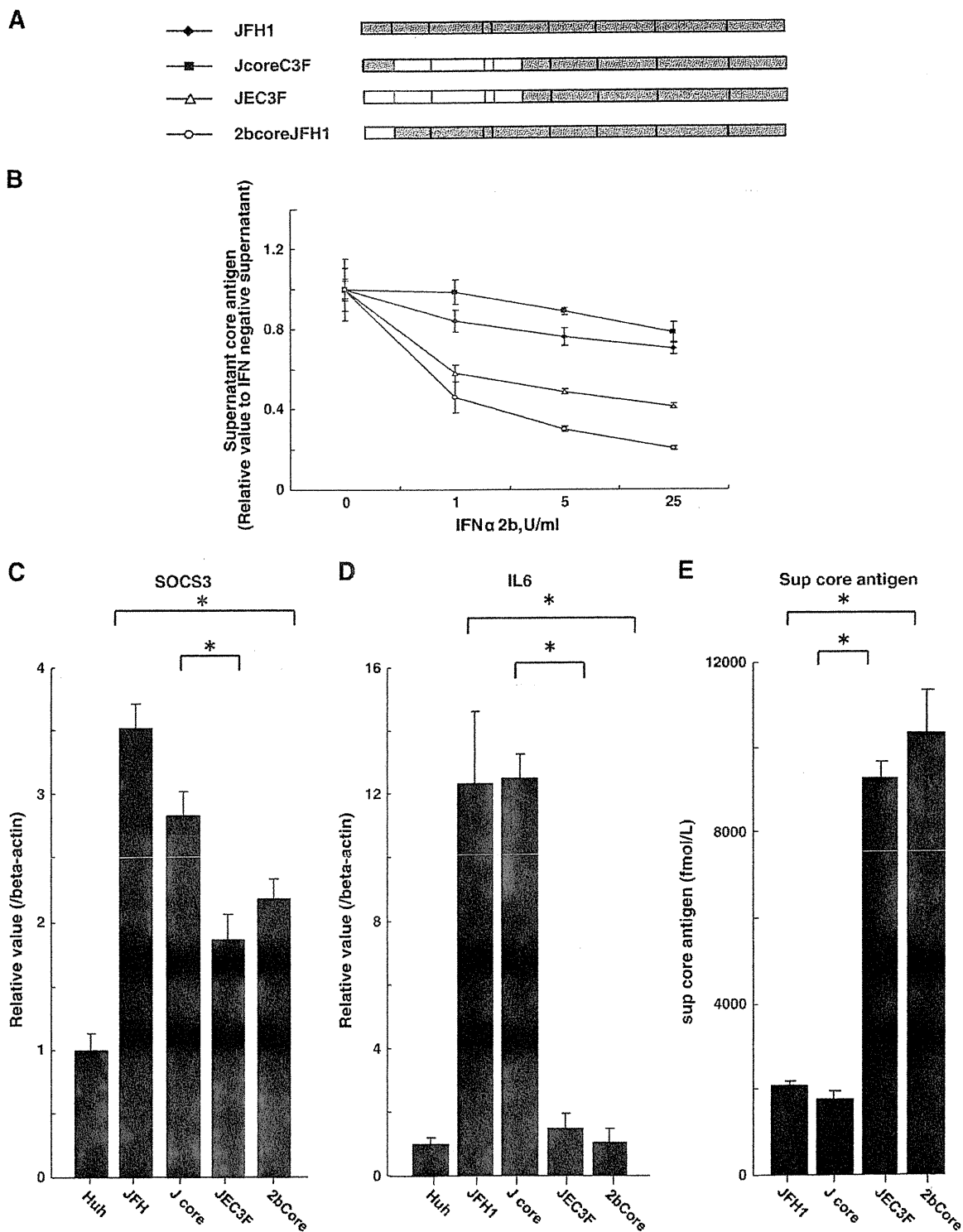


Fig. 7. Replacement of the HCV-2b-core region with JFH1-core causes upregulation of SOCS3 and IL-6 and restores resistance to IFN. **A.** Genome maps of JFH1, JEC3F, J core C3F, 2b core JFH1 recombinant cDNA. J core C3F was made by substitution of the core region of 2b/JFH1 with that of JFH1. The 2b core JFH1 was made by substitution of the core region of JFH1 with that of 2b/JFH1. **B.** Comparison of IFN-alpha sensitivity among JFH1 and JEC3F and core region substitution chimeric viruses. Ten μ g of J core C3F, 2b core JFH1, JEC3F, JFH1 RNA were transfected into 5×10^6 Huh7.5.1 cells and were divided into 12 wells. Forty eight hours after transfection, the cells were treated with 0, 1, 5 and 25 U/ml of IFN-alpha 2b. Seventy two hours after treatment, quantification of HCV core antigen was carried out in culture fluids. Assays were done in triplicate and the data are shown as mean \pm sd. Asterisks indicate p-values of less than 0.05. **C, D.** Core substitution leads to SOCS3 and IL-6 mRNA over-expression. Forty eight hours after transfection into cells, total RNA was isolated. Relative gene expression level SOCS3 (panel C) and IL6 (panel D) were determined by real time PCR. Values are shown as relative to those of uninfected Huh 751 cells. Assays were done in triplicate and the data are shown as mean \pm sd. Asterisks indicate p-values of less than 0.05. **E.** Change of secretion of core protein following core protein substitution. HCV RNA-transfected cells were divided into 12 wells. Five days after transfection, quantification of HCV core antigen was carried out in culture fluids. Assays were done in triplicate and the data are shown as mean \pm sd. Asterisks indicate p-values of less than 0.05.

5'-GGA GAA GCT GGA GAC TCA GGT G-3', SOCS1; forward, 5'-CACTTC CGC ACA TTC CGT TCG-3' and reverse, 5'-GAG GCC ATC TTC ACG CTA AGG-3', IL6; forward, 5'-GGT ACA TCC TCG ACG GCA TCT-3' and reverse, 5'-GTG CCT CTT TGC TGC TTT CAC-3', 25OAS; forward, 5'-CCA CCT TGG AAA GTG CCG ACA ATG CAG ACA-3' and reverse, 5'-CGA GTC TTT AAA AGC GAT TGC CAG ATG ATC -3', MxA; forward, 5'-GCC AGC AGC TTC AGA AGG CCA TGC TGC AGC -3' and reverse, 5'-GGG CAA GCC GGC GCC GAG CCT GCG TCA GCC -3'.

The siRNAs

The siRNAs directed against SOCS3 were designed as follows: SOCS3-HSS113312 stealth (sequence 5'- CCC AGA AGA GCC UAU UAC AUC UAC U-3' and 5'-AGU AGA UGU AAU AGG CUC UUC UGG G-3', Invitrogen) was used. 10 µg in vitro-synthesized HCV-RNA and 80 pmol siRNA SOCS3-HSS113312 or MOCK or control siRNA (negative universal control Med #2, Invitrogen) were electroporated into 5 × 10 naïve Huh7.5.1 cells using the protocol described in *HCV cell culture system*. Forty-eight hours after transfection, expression levels of SOCS3 mRNA were measured by real-time PCR. The difference in IFN sensitivity between SOCS3 knock down HCV infected cells and control HCV infected cells was determined by measuring supernatants HCV core antigen 72 hours after addition of IFN.

Immunohistochemistry for HCV core

HCV-JFH1 transfected or infected Huh7.5.1 cells were cultured on 22 mm-round micro cover glasses (Matsunami, Tokyo, Japan). For detection of HCV core, cells were fixed with cold acetone for 15 min. The cells were incubated with the primary antibodies for 1 hour at 37 °C, and with Alexa Fluor 488 goat anti-mouse IgG antibody (Molecular Probes, Eugene, OR) for 1 hour at room temperature. Cells were mounted with VECTA SHIELD Mounting Medium and DAPI (Vector Laboratories, Burlingame, CA) and visualized by fluorescence microscopy (BZ-8000, KEYENCE, Osaka, Japan).

Western blot analysis

Western blotting was performed as described (Tanabe et al., 2004). Briefly, 10 µg of total cell lysate was separated by SDS-PAGE, and blotted onto a polyvinylidene fluoride (PVDF) membrane. The membrane was incubated with the primary antibodies followed by a peroxidase-labeled anti IgG antibody, and was visualized by chemiluminescence using the ECL Western Blotting Analysis System (Amersham Biosciences, Buckinghamshire, UK).

Statistical analyses

Statistical analyses were performed using Student's *t*-test; *p*-values of less than 0.05 were considered statistically significant.

Acknowledgments

We thank Dr. Frank Chisari for providing Huh7.5.1 cells and Dr. Takaji Wakita for providing pJFH1fill. This study was supported by grants from Ministry of Education, Culture, Sports, Science and Technology-Japan, the Japan Society for the Promotion of Science, Ministry of Health, Labour and Welfare-Japan, Japan Health Sciences Foundation, and National Institute of Biomedical Innovation.

Appendix A. Supplementary data

Supplementary Fig. 1. Infectivity of the full-length 2b HCV RNA and 2b/JFH1 chimeric virus, JEC3F. A. Challenge of human liver-engrafted albumin-uPA/SCID mice with culture fluid from JFH1 and JEC3F cells. Cell culture fluids from the JFH1 clone and JEC3F were injected

intravenously into human liver engrafted albumin-uPA/SCID mice. Serum samples were obtained from the mice every 2 weeks after injection and the HCV RNA titer was determined. B. Fig. 1B Challenge of human liver-engrafted albumin-uPA/SCID mice by intrahepatic injection of in vitro synthesized, full-length 2b HCV RNA. Five hundred µl of RNA solution containing 30 µg of in vitro synthesized full-length 2b HCV RNA was injected into the livers of anesthetized chimeric mice through a small abdominal incision. Serum samples were obtained from the mice every 2 weeks after injection and the HCV RNA titer was determined.

Supplementary Fig. 2. Comparisons of replication efficiency of JFH1 and J6/JFH1, 2b/JFH1 chimeras after transfection into Huh7.5.1-cells. A. Structures of the J6/JFH1 and 2b/JFH1 genomes. J6 is joined between NS2 and NS3 with JFH1. 2b-HCV is joined with JFH1 within NS2 at nt. 2867. B. Measurements of core protein in cell culture fluids. Ten µg of JFH1, J6/JFH1, 2b/JFH1 RNA were transfected into 5 × 10⁶ Huh7.5.1 cells and the cells were cultured in 100 mm-diameter plates. The culture fluids from JFH1, J6/JFH1, H77/JFH1 or 2b/JFH1-transfected Huh7.5.1 cells were collected separately on the days indicated and the levels of core antigen were measured. These experiments were done three times with similar results independently. Panel B shows representative data.

Supplementary Fig. 3. Inhibition of infection by blocking CD81. Huh 7.5.1 cells were plated into a 6 well plate at 1.4 × 10⁵ cells per well. After 48 hours, the cells were incubated with anti-CD81 or isotypematched control antibody at the concentration indicated for 1 hour. Subsequently, cells were infected with 1 ml of JEC3F stock cell culture fluids at day 2 for 4 hours and washed with PBS. 48 hours after inoculation, anti-core immunostaining was performed with mouse anti-HCV core protein monoclonal antibody (Panels B and C). Quantification of HCV core antigen was carried out in culture fluids at 48 hours after infection (Panel A).

Supplementary Fig. 4. Comparison between 2b and JFH-1 core amino acid sequence.

Note: Supplementary materials related to this article can be found online at doi:10.1016/j.virol.2010.07.041.

References

- Alter, M.J., 1997. Epidemiology of hepatitis C. *Hepatology* 26 (3 Suppl 1), 62S–65S.
- Blight, K.J., Kolykhalov, A.A., Rice, C.M., 2000. Efficient initiation of HCV RNA replication in cell culture. *Science* 290 (5498), 1972–1974.
- Bode, J.G., Ludwig, S., Ehrhardt, C., Albrecht, U., Erhardt, A., Schaper, F., Heinrich, P.C., Haussinger, D., 2003. IFN- α antagonistic activity of HCV core protein involves induction of suppressor of cytokine signaling-3. *FASEB J.* 17 (3), 488–490.
- Bukh, J., Miller, R.H., Purcell, R.H., 1995. Genetic heterogeneity of hepatitis C virus: quasispecies and genotypes. *Semin. Liver Dis.* 15 (1), 41–63.
- Chang, K.C., Hansen, E., Foroni, L., Lida, J., Goldspink, G., 1991. Molecular and functional analysis of the virus- and interferon-inducible human MxA promoter. *Arch. Virol.* 117 (1–2), 1–15.
- Fried, M.W., Shiffman, M.L., Reddy, K.R., Smith, C., Marinos, G., Goncalves Jr., F.L., Haussinger, D., Diago, M., Carosi, G., Dhumeaux, D., Craxi, A., Lin, A., Hoffman, J., Yu, J., 2002. Peginterferon alfa-2a plus ribavirin for chronic hepatitis C virus infection. *N. Engl. J. Med.* 347 (13), 975–982.
- Gottwein, J.M., Scheel, T.K., Hoegh, A.M., Lademann, J.B., Eugen-Olsen, J., Lisby, G., Bukh, J., 2007. Robust hepatitis C genotype 3a cell culture releasing adapted intergenotypic 3a/2a (SS2/JFH1) viruses. *Gastroenterology* 133 (5), 1614–1626.
- Gottwein, J.M., Scheel, T.K., Jensen, T.B., Lademann, J.B., Prentoe, J.C., Knudsen, M.L., Hoegh, A.M., Bukh, J., 2009. Development and characterization of hepatitis C virus genotype 1-7 cell culture systems: role of CD81 and scavenger receptor class B type I and effect of antiviral drugs. *Hepatology* 49 (2), 364–377.
- Hanada, T., Kinjyo, I., Inagaki-Ohara, K., Yoshimura, A., 2003. Negative regulation of cytokine signaling by CIS/SOCS family proteins and their roles in inflammatory diseases. *Rev. Physiol. Biochem. Pharmacol.* 149, 72–86.
- He, Y., Katze, M.G., 2002. To interfere and to anti-interfere: the interplay between hepatitis C virus and interferon. *Viral Immunol.* 15, 95–119.
- Hoffmann, M., Zeisel, M.B., Jilg, N., Paranhos-Baccala, G., Stoll-Keller, F., Wakita, T., Hafkemeyer, P., Blum, H.E., Barth, H., Henneke, P., Baumert, T.F., 2009. Toll-Like Receptor 2 Senses Hepatitis C Virus Core Protein but Not Infectious Viral Particles. *J. Innate Immun.* 1 (No. 5), 446–454.
- Hoofnagle, J.H., di Bisceglie, A.M., 1997. The treatment of chronic viral hepatitis. *N. Engl. J. Med.* 336 (5), 347–356.
- Itsui, Y., Sakamoto, N., Kakinuma, S., Nakagawa, M., Sekine-Osajima, Y., Tasaka-Fujita, M., Nishimura-Sakurai, Y., Suda, G., Karakama, Y., Yamamoto, M., Watanabe, T.,

- Ueyama, M., Funaoka, Y., Azuma, S., Watanabe, M., 2009. Antiviral effects of the interferon-induced protein GBP-1 and its interaction with the hepatitis C virus NS5B protein. *Hepatology* 50 (6), 1727–1737.
- Itsui, Y., Sakamoto, N., Kurosaki, M., Kanazawa, N., Tanabe, Y., Koyama, T., Takeda, Y., Nakagawa, M., Kakinuma, S., Sekine, Y., Maekawa, S., Enomoto, N., Watanabe, M., 2006. Expressional screening of interferon-stimulated genes for antiviral activity against hepatitis C virus replication. *J. Viral Hepat.* 13 (10), 690–700.
- Jensen, T.B., Gottwein, J.M., Scheel, T.K., Hoegh, A.M., Eugen-Olsen, J., Bukh, J., 2008. Highly efficient JFH1-based cell-culture system for hepatitis C virus genotype 5a: failure of homologous neutralizing-antibody treatment to control infection. *J. Infect. Dis.* 198 (12), 1756–1765.
- Kalvakolanu, D.V., 2003. Alternate interferon signaling pathways. *Pharmacol. Ther.* 100 (1), 1–29.
- Kato, T., Date, T., Miyamoto, M., Furusaka, A., Tokushige, K., Mizokami, M., Wakita, T., 2003. Efficient replication of the genotype 2a hepatitis C virus subgenomic replicon. *Gastroenterology* 125 (6), 1808–1817.
- Kawaguchi, T., Yoshida, T., Harada, M., Hisamoto, T., Nagao, Y., Ide, T., Taniguchi, E., Kumemura, H., Hanada, S., Maeyama, M., Baba, S., Koga, H., Kumashiro, R., Ueno, T., Ogata, H., Yoshimura, A., Sata, M., 2004. Hepatitis C virus down-regulates insulin receptor substrates 1 and 2 through up-regulation of suppressor of cytokine signaling 3. *Am. J. Pathol.* 165 (5), 1499–1508.
- Lin, W., Choe, W.H., Hiasa, Y., Kamegaya, Y., Blackard, J.T., Schmidt, E.V., Chung, R.T., 2006. Hepatitis C virus core protein blocks interferon signaling by degrading STAT1. *Gastroenterology* 128 (4), 1034–1041.
- Lin, W., Kim, S.S., Yeung, E., Kamegaya, Y., Blackard, J.T., Kim, K.A., Holtzman, M.J., Chung, R.T., 2006. Hepatitis C virus core protein blocks interferon signaling by interaction with the STAT1 SH2 domain. *J. Virol.* 80 (18), 9226–9235.
- Lindenbach, B.D., Evans, M.J., Syder, A.J., Wolk, B., Tellinghuisen, T.L., Liu, C.C., Maruyama, T., Hynes, R.O., Burton, D.R., McKeating, J.A., Rice, C.M., 2005. Complete replication of hepatitis C virus in cell culture. *Science* 309 (5734), 623–626.
- Lohmann, V., Korner, F., Koch, J., Herian, U., Theilmann, L., Bartenschlager, R., 1999. Replication of subgenomic hepatitis C virus RNAs in a hepatoma cell line. *Science* 285 (5424), 110–113.
- Malaguarnera, M., Di Fazio, I., Romeo, M.A., Restuccia, S., Laurino, A., Trovato, B.A., 1997. Elevation of interleukin 6 levels in patients with chronic hepatitis due to hepatitis C virus. *J. Gastroenterol.* 32 (2), 211–215.
- Miyaaki, H., Ichikawa, T., Nakao, K., Matsuzaki, T., Muraoka, T., Honda, T., Takeshita, S., Shibata, H., Ozawa, E., Akiyama, M., Miura, S., Eguchi, K., 2009. Predictive value of suppressor of cytokine signal 3 (SOCS3) in the outcome of interferon therapy in chronic hepatitis C. *Hepatology* 49 (9), 850–855.
- Morikawa, K., Zhao, Z., Date, T., Miyamoto, M., Murayama, A., Akazawa, D., Tanabe, J., Sone, S., Wakita, T., 2007. The roles of CD81 and glycosaminoglycans in the adsorption and uptake of infectious HCV particles. *J. Med. Virol.* 79 (6), 714–723.
- Mozer-Lisewska, I., Sluzewski, W., Kaczmarek, M., Jenek, R., Szczepanski, M., Figlerowicz, M., Kowala-Piaskowska, A., Zeromski, J., 2005. Tissue localization of Toll-like receptors in biopsy specimens of liver from children infected with hepatitis C virus. *Scand. J. Immunol.* 62 (4), 407–412.
- Murayama, A., Date, T., Morikawa, K., Akazawa, D., Miyamoto, M., Kaga, M., Ishii, K., Suzuki, T., Kato, T., Mizokami, M., Wakita, T., 2007. The NS3 helicase and NS5B-to-3'X regions are important for efficient hepatitis C virus strain JFH-1 replication in Huh7 cells. *J. Virol.* 81 (15), 8030–8040.
- Pietschmann, T., Kaul, A., Koutsoudakis, G., Shavinskaya, A., Kallis, S., Steinmann, E., Abid, K., Negro, F., Dreux, M., Cosset, F.L., Bartenschlager, R., 2006. Construction and characterization of infectious intragenotypic and intergenotypic hepatitis C virus chimeras. *Proc. Natl. Acad. Sci. USA* 103 (19), 7408–7413.
- Polyak, S.J., Khabar, K.S., Rezeiq, M., Gretch, D.R., 2001. Elevated levels of interleukin-8 in serum are associated with hepatitis C virus infection and resistance to interferon therapy. *J. Virol.* 75 (13), 6209–6211.
- Ramadori, G., Christ, B., 1999. Cytokines and the hepatic acute-phase response. *Semin. Liver Dis.* 19 (2), 141–155.
- Ronni, T., Matikainen, S., Lehtonen, A., Palvimo, J., Dellis, J., Van Eylen, F., Goetschy, J.F., Horisberger, M., Content, J., Julkunen, I., 1998. The proximal interferon-stimulated response elements are essential for interferon responsiveness: a promoter analysis of the antiviral MxA gene. *J. Interferon Cytokine Res.* 18 (9), 773–781.
- Sabio, G., Das, M., Mora, A., Zhang, Z., Jun, J.Y., Ko, H.J., Barrett, T., Kim, J.K., Davis, R.J., 2008. A stress signaling pathway in adipose tissue regulates hepatic insulin resistance. *Science* 322 (5907), 1539–1543.
- Samuel, C., 2001. Antiviral actions of interferons. *Clin. Microbiol. Rev.* 14 (4), 778–809.
- Scheel, T.K., Gottwein, J.M., Jensen, T.B., Prentoe, J.C., Hoegh, A.M., Alter, H.J., Eugen-Olsen, J., Bukh, J., 2008. Development of JFH1-based cell culture systems for hepatitis C virus genotype 4a and evidence for cross-genotype neutralization. *Proc. Natl. Acad. Sci. USA* 105 (3), 997–1002.
- Sekine-Osajima, Y., Sakamoto, N., Mishima, K., Nakagawa, M., Itsui, Y., Tasaka, M., Nishimura-Sakurai, Y., Chen, C.H., Kanai, T., Tsuchiya, K., Wakita, T., Enomoto, N., Watanabe, M., 2008. Development of plaque assays for hepatitis C virus-JFH1 strain and isolation of mutants with enhanced cytopathogenicity and replication capacity. *Virology* 371 (1), 71–85.
- Song, M.M., Shuai, K., 1998. The suppressor of cytokine signaling (SOCS) 1 and SOCS3 but not SOCS2 proteins inhibit interferon-mediated antiviral and antiproliferative activities. *J. Biol. Chem.* 273 (52), 35056–35062.
- Tanabe, Y., Sakamoto, N., Enomoto, N., Kurosaki, M., Ueda, E., Maekawa, S., Yamashiro, T., Nakagawa, M., Chen, C.H., Kanazawa, N., Kakinuma, S., Watanabe, M., 2004. Synergistic inhibition of intracellular hepatitis C virus replication by combination of ribavirin and interferon- α . *J. Infect. Dis.* 189 (7), 1129–1139.
- Taniguchi, T., Ogasawara, K., Takaoka, A., Tanaka, N., 2001. IRF family of transcription factors as regulators of host defense. *Annu. Rev. Immunol.* 19, 623–655.
- Taniguchi, T., Takaoka, A., 2002. The interferon- α /beta system in antiviral responses: a multimodal machinery of gene regulation by the IRF family of transcription factors. *Curr. Opin. Immunol.* 14, 111–116.
- Taylor, D.R., Shi, S.T., Romano, P.R., Barber, G.N., Lai, M.M., 1999. Inhibition of the interferon-inducible protein kinase PKR by HCV E2 protein. *Science* 285 (5424), 107–110.
- Vlotides, G., Sorensen, A.S., Kopp, F., Zitzmann, K., Cengic, N., Brand, S., Zachoval, R., Auernhammer, C.J., 2004. SOCS-1 and SOCS-3 inhibit IFN- α -induced expression of the antiviral proteins 2, 5-OAS and MxA. *Biochem. Biophys. Res. Commun.* 320 (3), 1007–1014.
- Wakita, T., Pietschmann, T., Kato, T., Date, T., Miyamoto, M., Zhao, Z., Murthy, K., Habermann, A., Krausslich, H.G., Mizokami, M., Bartenschlager, R., Liang, T.J., 2005. Production of infectious hepatitis C virus in tissue culture from a cloned viral genome. *Nat. Med.* 11 (7), 791–796.
- Walsh, M.J., Jonsson, J.R., Richardson, M.M., Lipka, G.M., Purdie, D.M., Clouston, A.D., Powell, E.E., 2006. Non-response to antiviral therapy is associated with obesity and increased hepatic expression of suppressor of cytokine signalling 3 (SOCS-3) in patients with chronic hepatitis C, viral genotype 1. *Gut* 55 (4), 529–535.
- Zhu, H., Nelson, D.R., Crawford, J.M., Liu, C., 2005. Defective Jak-Stat activation in hepatoma cells is associated with hepatitis C viral IFN- α resistance. *J. Interferon Cytokine Res.* 25 (9), 528–539.

Comparison of HCV-associated gene expression and cell signaling pathways in cells with or without HCV replicon and in replicon-cured cells

Yuki Nishimura-Sakurai · Naoya Sakamoto · Kaoru Mogushi · Satoshi Nagaie · Mina Nakagawa · Yasuhiro Itsui · Megumi Tasaka-Fujita · Yuko Onuki-Karakama · Goki Suda · Kako Mishima · Machi Yamamoto · Mayumi Ueyama · Yusuke Funaoka · Takako Watanabe · Seishin Azuma · Yuko Sekine-Osajima · Sei Kakinuma · Kiichiro Tsuchiya · Nobuyuki Enomoto · Hiroshi Tanaka · Mamoru Watanabe

Received: 2 September 2009 / Accepted: 2 November 2009 / Published online: 12 December 2009
© Springer 2009

Abstract

Background Hepatitis C virus (HCV) replication is affected by several host factors. Here, we screened host genes and molecular pathways that are involved in HCV replication by comprehensive analyses using two genotypes of HCV replicon-expressing cells, their *cured* cells and naïve Huh7 cells.

Y. Nishimura-Sakurai and N. Sakamoto contributed equally to this work.

Electronic supplementary material The online version of this article (doi:10.1007/s00535-009-0162-3) contains supplementary material, which is available to authorized users.

Y. Nishimura-Sakurai · N. Sakamoto (✉) · M. Nakagawa · Y. Itsui · M. Tasaka-Fujita · Y. Onuki-Karakama · G. Suda · K. Mishima · M. Yamamoto · M. Ueyama · Y. Funaoka · T. Watanabe · S. Azuma · Y. Sekine-Osajima · S. Kakinuma · K. Tsuchiya · M. Watanabe
Department of Gastroenterology and Hepatology,
Tokyo Medical and Dental University, 1-5-45 Yushima,
Bunkyo-ku, Tokyo 113-8519, Japan
e-mail: nsakamoto.gast@tmd.ac.jp

N. Sakamoto · M. Nakagawa · S. Kakinuma
Department for Hepatitis Control,
Tokyo Medical and Dental University, Tokyo, Japan

K. Mogushi · S. Nagaie · H. Tanaka
Information Center for Medical Science,
Tokyo Medical and Dental University, Tokyo, Japan

Y. Itsui
Department of Internal Medicine,
Soka Municipal Hospital, Saitama, Japan

N. Enomoto
First Department of Internal Medicine,
University of Yamanashi, Yamanashi, Japan

Methods Huh7 cell lines that stably expressed HCV genotype 1b or 2a replicon were used. The *cured* cells were established by treating HCV replicon cells with interferon-alpha. Expression of 54,675 cellular genes was analyzed by GeneChip DNA microarray. The data were analyzed by using the KEGG Pathway database.

Results Hierarchical clustering analysis showed that the gene-expression profiles of each cell group constituted clear clusters of naïve, HCV replicon-expressed, and cured cell lines. The pathway process analysis between the replicon-expressing and the *cured* cell lines identified significantly altered pathways, including MAPK, steroid biosynthesis and TGF-beta signaling pathways, suggesting that these pathways were affected directly by HCV replication. Comparison of *cured* and naïve Huh7 cells identified pathways, including steroid biosynthesis and sphingolipid metabolism, suggesting that these pathways were required for efficient HCV replication. Cytoplasmic lipid droplets were obviously increased in replicon-expressing and *cured* cells as compared to naïve cells. HCV replication was significantly suppressed by peroxisome proliferator-activated receptor (PPAR)-alpha agonists but augmented by PPAR-gamma agonists.

Conclusion Comprehensive gene expression and pathway analyses show that lipid biosynthesis pathways are crucial to support proficient virus replication. These metabolic pathways could constitute novel antiviral targets against HCV.

Keywords DNA microarray · KEGG database · HCV replicon · Lipid metabolism

Abbreviations

HCV Hepatitis C virus
TLR Toll-like receptor
BMP Bone morphogenetic protein

TGF	Transforming growth factor
FKBP	FK-binding protein
HSP	Heat shock proteins
FBS	Fetal bovine serum
YFP	Yellow fluorescence protein
FACS	Fluorescent activated cell sorting
RIN	RNA integrity number
SAM	Significance analysis of microarray
KEGG	Kyoto Encyclopedia of Genes and Genomes
EGID	NCBI Entrez Gene ID
RT-PCR	Reverse transcription-polymerase chain reaction
MTS	Dimethylthiazol carboxymethoxyphenyl sulfophenyl tetrazolium
PPAR	Peroxisome proliferator-activated receptor

Introduction

Hepatitis C virus (HCV) infection is one of the most important causative agents of acute and chronic hepatitis, liver cirrhosis and hepatocellular malignancies [1]. Currently, the most efficient combination treatment of ribavirin plus peginterferon can eliminate the virus in almost half of the patients treated [2, 3]. Thus, it is our high priority goal to understand the HCV life cycle precisely, to identify cellular cofactors for HCV replication and to develop new class antiviral therapeutics.

Molecular analyses of the HCV life cycle, virus–host interactions, and mechanisms of liver cell damage by the virus are not understood completely, mainly because of the lack of cell culture systems. These problems have been partly overcome by the development of the HCV subgenomic replicon [4] and HCV cell culture systems [5, 6]. These systems have allowed us to study the complete HCV life cycle: virus-cell entry, translation, protein processing, RNA replication, virion assembly and virus release.

Several host proteins and drugs have been reported to have a direct affect on HCV replication in vitro [7]. These include factors that affect immune responses (interferons and their related genes [8, 9], RIG-I, TLRs [10]), cell proliferation (BMP7 [11], TGF-beta [12], nucleolin [13]), molecular chaperone function (cyclophilin [14], ER-stress proteins [15], FKBP [16], HSP27 [17], HSP90 [18]) and lipid metabolism (cholesterol, sphingolipid [19]). However, it is often difficult to determine whether these genes are changed by HCV replication or the changes are essential for HCV replication in the host cells.

In this study, we investigated the effects of host cellular gene expression using our HCV replicon system [20, 21]. We performed DNA microarray analyses using cells expressing the replicons, the corresponding *cured* cells, from which the replicon had been eliminated by prolonged treatment with interferon-alpha, and naïve Huh7 cells. Furthermore, we investigated the signaling pathways using DNA microarrays to study molecular pathways that are involved in the HCV life cycle and its pathogenesis.

Materials and methods

Cells and cell culture

Huh7 cells were maintained in Dulbecco's modified minimal essential medium (Sigma, St. Louis, MO) supplemented with 10% fetal calf serum at 37°C under 5% CO₂. To maintain cell lines carrying the HCV replicon (Huh7/Rep cells), G418 (Nakalai Tesque, Kyoto, Japan) was added to the culture medium to a final concentration of 500 µg/ml.

HCV replicon and cell culture

The HCV-1b replicon plasmid, pHCV1bneo-delS, was provided by Dr. Christoph Seeger (Fox Chase Cancer Center, Philadelphia, PA) [22]. HCV-2a replicon plasmid, pSGR-JFH1, was provided by Dr. Takaji Wakita (National Institute of Infectious Diseases, Tokyo, Japan). The neomycin phosphotransferase (Neo) gene of pHCV1bneo-delS and pSGR-JFH1 was replaced by a chimeric gene coding for yellow fluorescent protein fused in-frame with the foot-and-mouth disease virus peptide 2A (P2A) autocleavage motif followed by neomycin phosphotransferase, which we designated *Yeo* (Fig. 1) [23]. An HCV *Feo*-replicon that expresses chimeric firefly luciferase and the neomycin resistance gene has been described [20, 21]. In vitro replicon RNA synthesis, RNA transfection and selection of G418-resistant cell lines were carried out as described previously [21, 24]. Briefly, replicon RNAs were transfected into Huh7 cells. By cell culture in the presence of G418, we established Huh7 cell lines that stably express the *Yeo*-replicons: Huh7/Rep-1b-*Yeo* and Huh7/Rep-2a-*Yeo*.

Fluorescence microscopy and FACS analysis

The cells were plated onto eight-well chamber slides (Lab-Tek® Chamber Slide™ System, Nalgen Nunc International, Rochester, NY), and the YFP expression was detected by fluorescence microscopy (BZ-8000,

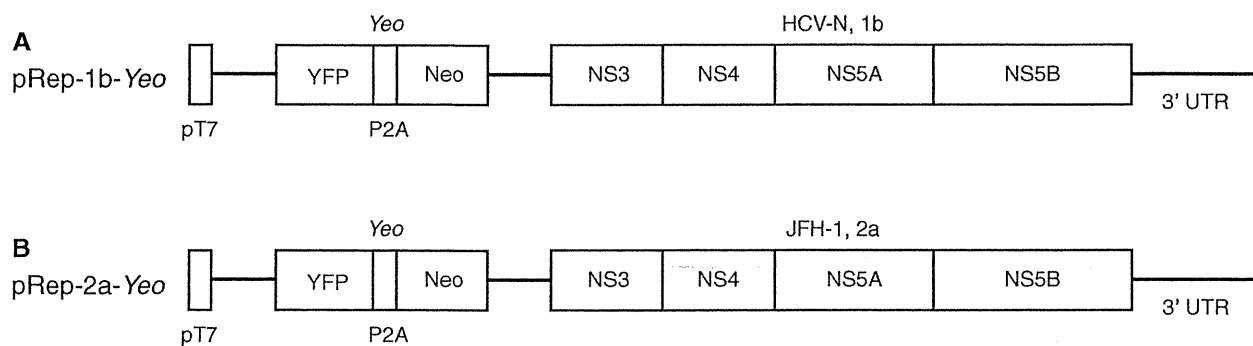


Fig. 1 Structure of replicon plasmid constructs. A hepatitis C virus (HCV) replicon plasmid, pRep-1b-Yeo (a) and pRep-2a-Yeo (b), was reconstructed from pHCV1bneo-delS [22] and pSGR-JFH1 [47] by replacing the neomycin phosphotransferase (Neo) gene with a fusion

gene of yellow fluorescence protein (YFP) and Neo, which we designate “Yeo.” NS Nonstructural region, pT7 T7 promoter, 3' UTR 3'untranslated region, P2A foot-and-mouth disease peptide 2A (see also “Materials and methods”) [23]

KEYENCE, Osaka, Japan) and FACS Caliber using CellQuest software (BD Biosciences, Franklin Lakes, NJ).

manufacturer's instructions. Assays were performed in duplicate.

Cell sorting

Analysis of gene expression data

Cells were treated for 5 min with trypsin/EDTA at 37°C and then resuspended in 10% FBS/DMEM. A single cell suspension was prepared by passage through a 35- μ m nylon filter. The cell populations that support a high level of Yeo-replicon expression (Huh7/Rep-1b-Yeo^{high} and Huh7/Rep-2a-Yeo^{high}) were separated using a FACS Vantage SE cell-sorting system (BD Biosciences). The YFP-directed fluorescence of sorted cells was confirmed by fluorescence microscopy and FACS.

A total of ten microarray datasets was normalized using the robust multi-array average (RMA) method under R 2.8.1 statistical software (<http://www.R-project.org>). Estimated gene expression levels were \log_2 -transformed, data from 62 control probe sets were removed, and we selected 18,613 probe sets that were categorized as “present” or “marginal” among all samples. We performed two sets of gene comparisons to examine effects of HCV replicons on host cellular gene expression: one was the high Yeo-replicon-expressing cells versus cured cells and the other was parental Huh7 cells versus cured cells. We selected differently expressed genes using the significance analysis of microarray (SAM) as described by Tusher et al. [27], and the fold changes and the *Q*-values were calculated for each probe sets. We used $\delta = 0.1$ as a cutoff parameter for SAM. A hierarchical clustering with selected genes was performed with R software. Euclidean distance was used to calculate the similarity matrix among genes or cell conditions, respectively. The complete linkage method was used for agglomeration.

Establishment of the cured Huh7 cells

Molecular pathway analysis and visualization of gene expression data

Cured Huh7 cells (cHuh7) were established by eliminating the HCV replicon from the Yeo-1b^{high} and -2a^{high} replicon expressing Huh7 cells by treatment with 100 U/ml of interferon-alpha for 14 days [6, 25]. Clearance of replicon RNA was confirmed by FACS analysis and by the loss of resistance to G418.

RNA preparation and microarray hybridization

We used the KEGG Pathway database to investigate the molecular reactions and pathways that showed significant gene expression changes [28]. The KEGG Pathway is a database of biological systems, consisting of over 4,252 genes and 204 molecular pathway-wiring diagrams of interaction and reaction networks (<http://www.genome.jp/kegg/pathway.html>). Prior to the pathway analysis, we selected probe sets that were differentially expressed

Total cellular RNA was extracted from the 1b^{high} and 2a^{high} Yeo-replicon cells, cured-1b and -2a cells and naïve Huh7 cells using ISOGEN (Wako). Integrity of obtained RNA was assessed using Agilent 2100 Bioanalyzer (Agilent Technologies, Palo Alto, CA). All samples had an RNA Integrity Number (RIN) greater than 9.4 [26]. Complementary RNA was prepared from 1 μ g total RNA, using one-cycle target labeling and a control reagents kit (Affymetrix, Santa Clara, CA). Hybridization and signal detection of the Human Genome U133 Plus 2.0 array (Affymetrix) were performed in accordance with the

between Huh7 and *cured* cells and between *cured* cells and replicon cells. For Huh7 versus *cured* cells analyses, we selected probe sets that showed 20% upregulation or downregulation (i.e., fold change of greater than 1.2) in both Huh7 versus *cured*-1b and Huh7 versus *cured*-2a cells. For replicon cell versus *cured* cell analyses, we selected probe sets that showed 20% upregulation or downregulation in both *cured*-1b versus replicon-1b cells or *cured*-2a versus replicon-2a cells. Association between the obtained gene list and each pathway was evaluated by Fisher's exact test. The significance level for KEGG analysis was set to a false discovery rate (FDR) of lower than 0.3 using the Benjamini and Hochberg method [29].

We next visualized functional associations between the differentially expressed genes and biological pathway processes. The KEGG Pathway provides a reference knowledge base for linking genomes to biological systems and also to environments by the processes of Pathway mapping and BRITE mapping. NCBI Entrez Gene IDs (EGIDs) for each gene in the pathways were extracted from the database. The relationship between probe sets on the microarray and EGIDs was obtained from a gene annotation file provided by Affymetrix. Thereafter, gene expression changes were mapped on the pathway by combining the results of fold-change analyses with the data sets above.

Real-time PCR analysis of mRNA expression

To confirm the results of the microarray analysis, we examined the expression levels of several mRNA by real-time RT-PCR (7500 Real Time PCR Systems, Applied Biosystems, Foster City, CA). Single-stranded cDNA was synthesized from total RNA using SuperScript II reverse transcriptase (Invitrogen) and random hexamers (Takara Bio Inc., Shiga, Japan) as primers. Expression of mRNA was quantified using QuantiTect SYBR Green PCR master Mix (QIAGEN, Valencia, CA). The primers used were as follows: HMGCR, SQLE, CYP51A1, TM7SF2, NSDHL, EBP and beta-actin. The nucleotide sequences of primers and corresponding product sizes are as indicated (see Supplementary Table 1).

Oil red O staining

Huh7 cells, replicon cells and *cured* cells were cultured on 18-mm-round micro cover glasses (Matsunami, Tokyo, Japan). These cells were fixed with 4% paraformaldehyde for 5 min at room temperature. After washing with PBS, the cells were permeabilized with 0.05% Triton X-100 in PBS for 5 min at room temperature. Staining of intracellular neutral lipids was performed with Oil red O, and nuclei were stained with Mayer's hematoxylin using Oil

red O stain kit procedure (Diagnostic Biosystems Inc., Pleasanton, CA).

Immunofluorescence analysis

Huh7 cells, replicon cells and *cured* cells were cultured on 18-mm-round micro cover glasses. For immunostaining, the cells were fixed in 4% paraformaldehyde for 5 min at room temperature. For detection of HCV-NS5A, cells were incubated with the primary antibody (Bioscience International, Saco, ME) for 1 h at 37°C. The fluorescent secondary antibodies were Alexa Fluor 594 goat anti-mouse IgG antibody (Invitrogen, Carlsbad, CA). Nuclei were labeled with 4',6-diamidino-2-phenylindole (DAPI). Lipid droplets were visualized with BODIPY 493/503 (Invitrogen). Analysis was performed on a Delta-Vision microscope system (Applied Precision, Seattle, WA).

Luciferase-based expression analysis of HCV replicon and analysis of cell viability

Huh7/Rep-Feo cells [20, 21] were cultured with various concentrations of peroxisome proliferator-activated receptor (PPAR)-alpha and -gamma agonists. After 48 h of culture, levels of HCV replication were quantified by internal luciferase assay using a Bright-Glo Luciferase Assay System (Promega). Assays were performed in triplicate, and the results were expressed as mean \pm SD as percentages of the controls. To evaluate cell viability, dimethylthiazol carboxymethoxyphenyl sulfophenyl tetrazolium (MTS) assay was performed using a Cell Titer 96 Aqueous One Solution Cell Proliferation Assay (Promega) according to manufacturer's directions.

Statistical analyses

Statistical analyses were performed using the Student's *t*-test, and *P*-values of less than 0.05 were considered as statistically significant.

Results

Fluorescence detection of Yeo replicon

Genotypes 1b and 2a *Yeo*-replicon RNAs were stably transfected into Huh7 cells (Huh7/Rep-1b-Yeo and Huh7/Rep-2a-Yeo, respectively, Fig. 1). In these transfected cells, expression of the HCV replicon was visualized by HCV-IRES-driven, YFP-mediated fluorescence (Fig. 2, left panels). The expression levels of individual cells could be measured by fluorescence intensity and cytogram analysis using flow cytometry (Fig. 2, right panels).

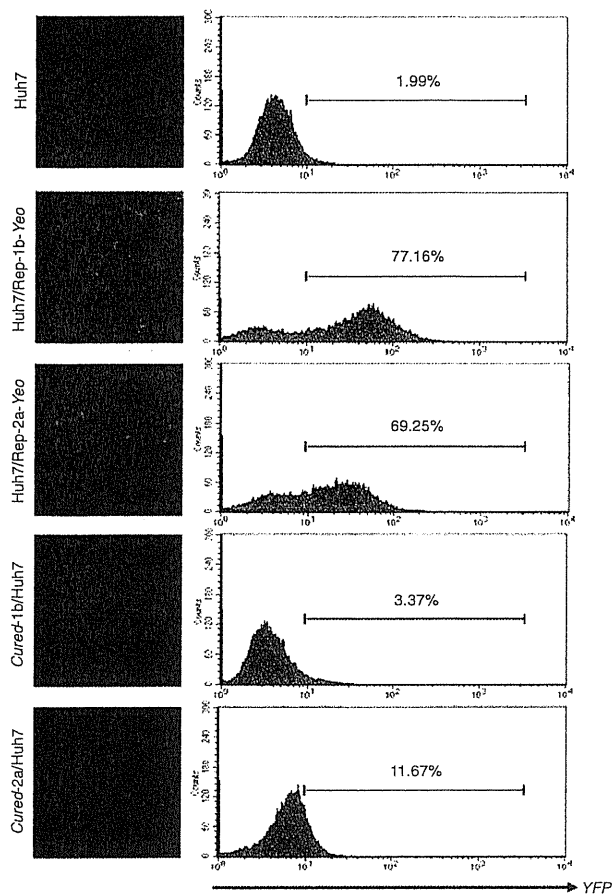


Fig. 2 Visualization of YFP replicon expression. Detection of YFP expression by fluorescence microscopy analysis and of intracellular YFP expression by FACS analysis

Our initial trial was to compare gene expression profiles between replicon-expressing cells and parental Huh7 cells. However, these comparisons identified gene expressional changes induced by HCV infection and by adaptation of the host cell to support efficient HCV replication, because transfection of replicon RNA and G418-treatment of cells resulted in selection of a cell population that can support a high level of HCV subgenomic replication. Therefore, we used *cured* cell lines, which were established from Huh7/Rep-1b-Yeo and -2a-Yeo by interferon-alpha treatment. These cured cell lines are highly permissive for HCV replication on re-introduction of virus or replicon RNA (Fig. 2). With these backgrounds, we performed two sets of gene comparison using microarray analyses: comparison of replicon-expressing cell lines (Huh7/Rep-1b-Yeo and Huh7/Rep-2a-Yeo) and *cured* cells (Cured-1b/Huh7 and Cured-2a/Huh7) was intended to identify genes that are affected by HCV replication, and comparison of parental Huh7 cells and *cured* cell lines was intended to identify

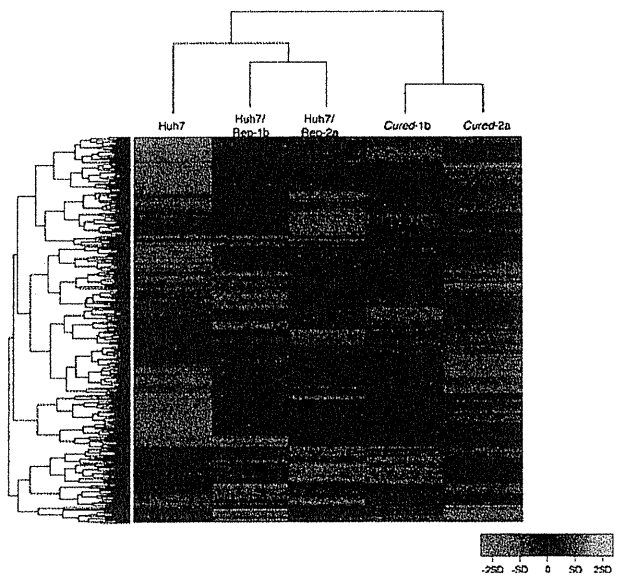


Fig. 3 Hierarchical clustering of gene expression profiles obtained from the 1b and 2a Yeo-replicon expressing cells, cured cells and Huh7. The 1,870 probe sets that changed expression more than 1.2-fold in either Huh7 versus *cured* or *cured* versus replicon were selected. Dendrograms show the classification determined by hierarchical clustering analysis. *Red* and *green* colors indicate relative overexpression and underexpression, respectively

genes that are essential for a high level of HCV replication in cultured cells.

Hierarchical clustering gene expression profiles in naïve, replicon-expressing and cured cells

Datasets from the microarrays were normalized using the robust multi-array average (RMA) method, and differentially expressed genes were extracted in replicon cells, *cured* cells and naïve Huh7 cells. Gene expression profiles were well correlated each other between duplicate microarray data from the same cell line with the Pearson's correlation coefficients (R^2) of greater than 0.975 (see Supplementary Fig. 1). In this analysis, 1,870 probe sets showed differences in expression levels of more than 1.2-fold under $\delta < 0.1$ in either Huh7 versus *cured* (1,516 probe sets) or *cured* versus replicon (372 probe sets). A hierarchical clustering analysis showed that the gene-expression profiles of each cell group constituted clear clusters, Huh7/Rep-2a and Huh7/Rep-1b, Cured-2a and Cured-1b, and Huh7 cells (Fig. 3). Among genes whose expression differed significantly between replicon-expressing cells and *cured* cells, 15 showed changes of more than two-fold (Table 1). These included cell cycle- or cell growth-related genes (nuclear protein 1, growth differentiation factor 15, urothelial cancer associated 1, inhibin and tubulin), oncogene (Ras-related GTP binding D) and interferon-related gene (IFIM3). On the other hand, 37

Table 1 Microarray analysis: genes for which the expression changed more than two-fold in Rep-1b/Huh7 and Rep-2a/Huh7 cells compared to their *cured* cells

Probe set	Title	Rep1b/ <i>cured</i> 1b		Rep2a/ <i>cured</i> 2a	
		Fold change	Q-value	Fold change	Q-value
209230_s_at	Nuclear protein 1	5.41	0.00	13.78	7.44
221523_s_at	Ras-related GTP binding D	3.82	0.00	2.32	24.60
221524_s_at	Ras-related GTP binding D	3.17	0.00	2.40	17.08
205923_at	Reelin	3.14	0.00	2.70	12.42
200924_s_at	Hypothetical protein LOC442497/solute carrier family 3 (activators of dibasic and neutral amino acid transport), member 2	2.84	0.00	2.63	0.69
221577_x_at	Growth differentiation factor 15	2.62	0.00	3.16	0.00
233030_at	Patatin-like phospholipase domain containing 3	2.07	0.00	2.31	3.16
201471_s_at	Sequestosome 1	2.52	0.81	2.10	2.45
227919_at	Urothelial cancer associated 1	5.09	0.90	2.90	54.18
207076_s_at	Argininosuccinate synthetase 1	2.99	0.90	2.22	61.28
205749_at	Cytochrome P450, family 1, subfamily A, polypeptide 1	2.69	0.90	2.63	4.55
217127_at	Cystathionase (cystathionine gamma-lyase)	2.32	3.05	2.38	6.54
210587_at	Inhibin, beta E	2.51	4.25	3.89	2.45
214023_x_at	Tubulin, beta 2B	2.41	4.25	4.31	54.18
212203_x_at	Interferon induced transmembrane protein 3 (1-8U)	2.34	5.75	2.09	54.18

genes were up-regulated by more than two-fold between *cured* and naïve cells (Table 2), which included genes such as chemokine (CCL14), solute carrier family and metallothionein family.

Pathway process analyses and hierarchical clustering of genes in each functional category

Using the KEGG Pathway database, we analyzed pathway processes that were altered between replicon-expressing cells and *cured* cells as well as between *cured* cells and Huh7 cells (Supplementary Tables 2, 3). Comparison of the pathway processes between replicon-expressing and *cured* cells identified six pathways that showed differences of FDR < 0.3, including pathways related to MAPK ($P = 4.0 \times 10^{-4}$, FDR 0.08), biosynthesis of steroids ($P = 4.21 \times 10^{-3}$, FDR 0.21) and TGF-beta ($P = 8.4 \times 10^{-3}$, FDR 0.29) (KEGG Pathway maps for each significant pathway are shown in Supplementary Fig. 2A–F). Comparison of the pathway processes between *cured* and naïve Huh7 cells identified 11 significant pathways (KEGG Pathway maps for each significant pathway are shown in Fig. 5 and Supplementary Fig. 3A–J). These included pathways that were related to TGF-beta ($P = 8.42 \times 10^{-3}$), cell cycle ($P = 9.0 \times 10^{-3}$) and sphingolipid metabolism ($P = 1.32 \times 10^{-2}$). Interestingly, there were significant changes in the biosynthesis of steroids ($P = 1.75 \times 10^{-4}$) between *cured* and naïve Huh7 cells. These results suggested that several lipid metabolism processes were substantially associated with efficient HCV replication in host cells.

Hierarchical clustering analyses of representative genes included in functional pathway categories

Based on pathway process analyses using the KEGG database, we performed hierarchical clustering analyses of each functional subset of genes (fold change > 1.2, Fig. 4a–c). The cell cycle, cholesterol biosynthesis and sphingolipid metabolism-related genes demonstrated clear clusters in replicon cells, *cured* cell and parental Huh7, respectively. In particular, cholesterol biosynthesis-related genes were activated in replicon cells and *cured* cells.

Mapping between pathway information and gene expression data

Knowing that cholesterol metabolism pathway was changed substantially in *cured* cells, we performed graphical mapping of the related genes to the KEGG Pathway map database (Fig. 5). Similar to the pathway analyses, cholesterol biosynthesis related genes, which are involved in the mevalonate pathway or sterol biosynthesis, were clearly activated in *cured* cells compared to naïve Huh7 (Fig. 5).

To verify the microarray results, we performed real-time RT-PCR of cholesterol biosynthesis-related genes including HMGCR, SQLE, NSDHL, CYP51A1, TM7SF2 and EBP. All the genes were upregulated in replicon-expressing and *cured* cells compared to the naïve Huh7 cells (Fig. 6). These results were consistent with the microarray data.

Table 2 Microarray analysis: genes for which the expression changed more than two-fold in *cured-1b* and *cured-2a* cells compared to Huh7

Probe set	Title	Cured1b/Huh7		Cured2a/Huh7	
		Fold change	Q-value	Fold change	Q-value
210390_s_at	Chemokine (C–C motif) ligand 14/15	4.49	0.00	2.56	0.00
221168_at	PR domain containing 13	2.38	0.00	2.15	0.00
1553995_a_at	5'-nucleotidase, ecto (CD73)	2.15	0.00	3.64	0.36
204897_at	Prostaglandin E receptor 4 (subtype EP4)	2.07	2.40	2.19	0.36
214522_x_at	Histone cluster 1, H2ad/H3d	3.01	4.12	2.98	0.46
214472_at	Histone cluster 1, H2ad/H3a-j	3.36	5.08	3.53	0.46
218280_x_at	Histone cluster 2, H2aa3/H2aa4	4.65	5.20	5.17	0.61
232035_at	Histone cluster 1, H4a-f, H4 h-l/histone cluster 2, H4a-b/histone cluster 4, H4	5.56	6.51	5.37	0.95
214455_at	Histone cluster 1, H2bc, H2be, H2bf, H2bg, H2bi	4.72	6.51	2.68	0.61
202708_s_at	Histone cluster 2, H2be	4.48	6.51	5.31	0.95
214290_s_at	Histone cluster 2, H2aa3/H2aa4	4.06	6.51	2.98	2.08
209398_at	Histone cluster 1, H1c	3.40	6.51	3.60	2.08
230795_at	–	2.91	6.51	4.51	0.95
1553994_at	5'-nucleotidase, ecto (CD73)	2.29	6.51	2.31	3.34
208180_s_at	Histone cluster 1, H4a-f, H4 h-l/histone cluster 2, H4a, H4b/histone cluster 4, H4	6.27	7.65	3.40	1.46
215779_s_at	Histone cluster 1, H2bc, H2be, H2bf, H2bg, H2bi	3.53	7.65	5.86	1.46
206110_at	–	3.82	9.12	10.68	0.00
206535_at	Solute carrier family 2 (facilitated glucose transporter), member 2	3.58	9.12	2.84	5.02
213880_at	Leucine-rich repeat-containing G protein-coupled receptor 5	2.81	9.12	3.02	5.02
210387_at	Histone cluster 1, H2bc, H2be, H2bf, H2bg, H2bi	3.24	10.68	2.28	11.66
203044_at	Chondroitin sulfate synthase 1	2.36	11.85	2.67	2.08
207102_at	Aldo-keto reductase family 1, member D1 (delta 4-3-ketosteroid-5-beta-reductase)	2.14	13.35	5.58	0.36
219596_at	THAP domain containing 10	2.20	16.73	3.32	2.08
217997_at	Pleckstrin homology-like domain, family A, member 1	2.15	23.48	3.01	3.34
217996_at	Pleckstrin homology-like domain, family A, member 1	2.12	23.48	2.21	11.66
217165_x_at	Metallothionein 1F	3.36	29.61	3.25	11.66
213629_x_at	Metallothionein 1F	3.13	29.61	3.70	11.66
210524_x_at	–	2.39	29.61	2.46	17.81
206143_at	Solute carrier family 26, member 3	2.35	29.61	2.49	17.81
212859_x_at	Metallothionein 1E	3.46	35.93	4.07	11.66
208581_x_at	Metallothionein 1X	3.31	35.93	3.52	17.81
204326_x_at	Metallothionein 1X	3.24	35.93	3.49	17.81
211456_x_at	Metallothionein 1 pseudogene 2	3.19	35.93	3.71	17.81
206461_x_at	Metallothionein 1H	3.09	35.93	3.49	17.81
216336_x_at	Metallothionein 1E, 1H, 1 M/metallothionein 1 pseudogene 2	3.02	35.93	3.27	17.81
212185_x_at	Metallothionein 2A	2.92	35.93	2.85	17.81
204745_x_at	Metallothionein 1G	2.73	35.93	3.31	17.81

Detection of intracellular lipid droplets in naïve, replicon-expressing and cured cells

Because several lipid-related pathways were extracted (Supplementary Tables 2 and 3), we examined phenotypes of the cell lines featuring different lipid metabolism

gene expression profiles by carrying out detection of cellular lipid droplets (Fig. 8a, b). The cells were stained by Oil red O or BODIPY493/503, dye solutions specific for neutral lipids. We found a large number of lipid droplets in the cytoplasm of each Huh7 cell line. The number of lipid droplets obviously was increased more in

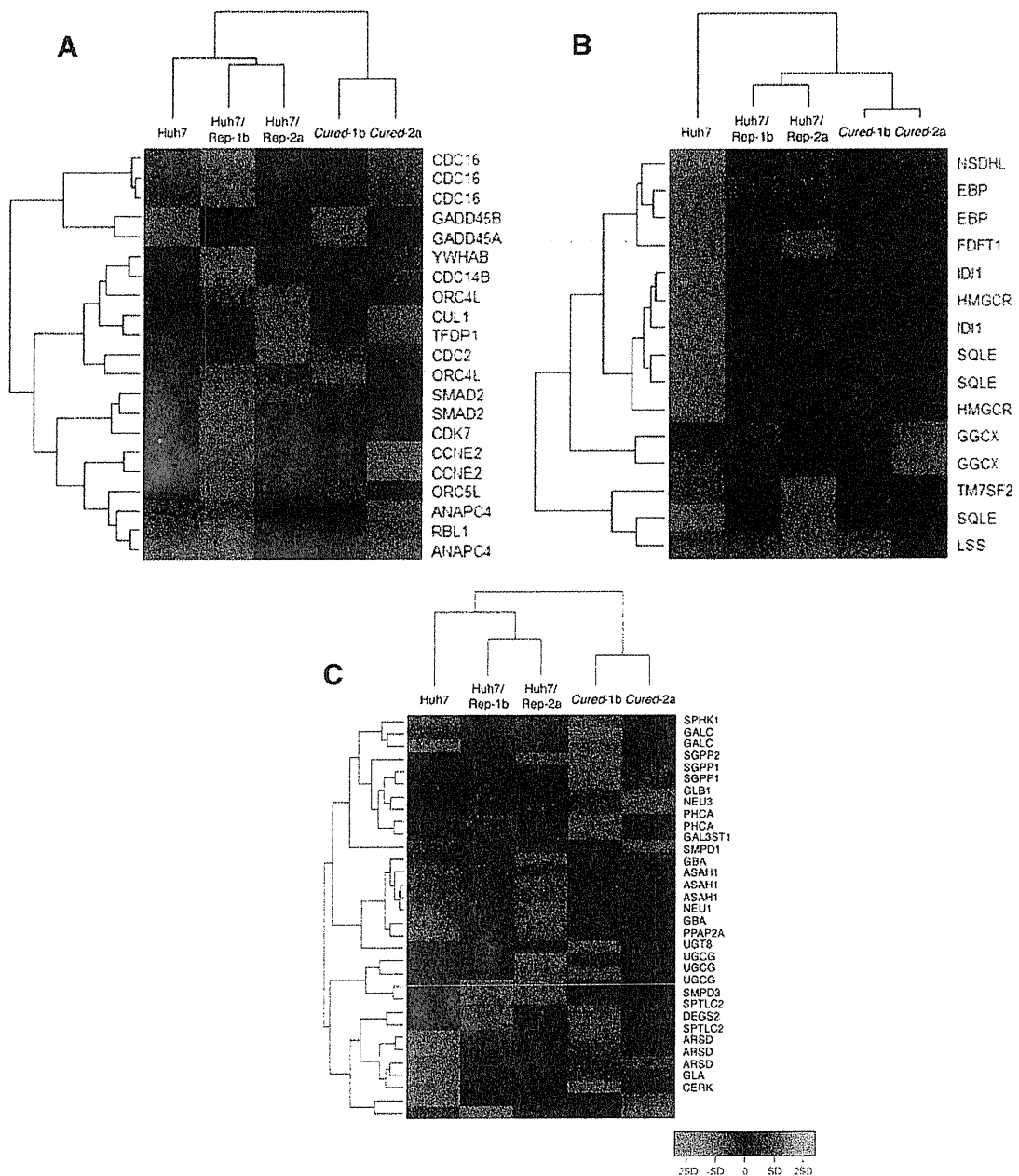


Fig. 4 Hierarchical clustering of representative genes included in each KEGG Pathway map. **a** Cell cycle, **b** cholesterol biosynthesis, **c** sphingolipid metabolism. Dendrograms shows the classification

determined by hierarchical clustering analysis. *Red* and *green* colors indicate relative overexpression and underexpression, respectively

the two replicon-expressing cells and the *cured* cells than in the parental Huh7 cells. Lipid and HCV-NS5A double staining showed an increase in lipid droplets in cells that expressed HCV proteins (Fig. 8b). Analyses of the KEGG fatty acid metabolism pathway showed that a substantial number of the genes of these pathways were up-regulated in the *cured* cells compared to the naïve cells, although these could not reach statistical significance (Fig. 7).

Effects of hepatitis C virus replication by PPAR-alpha and gamma agonists

To assess the effects of lipid metabolic status on the intracellular replication of the HCV genome, Huh7/Rep-Feo cells were cultured with various concentrations of several PPAR-alpha agonists (clofibrate, fenofibrate and bezafibrate) and gamma agonists (pioglitazone and troglitazone) (Fig. 9). The luciferase activities of the Huh7/

BIOSYNTHESIS OF STEROIDS

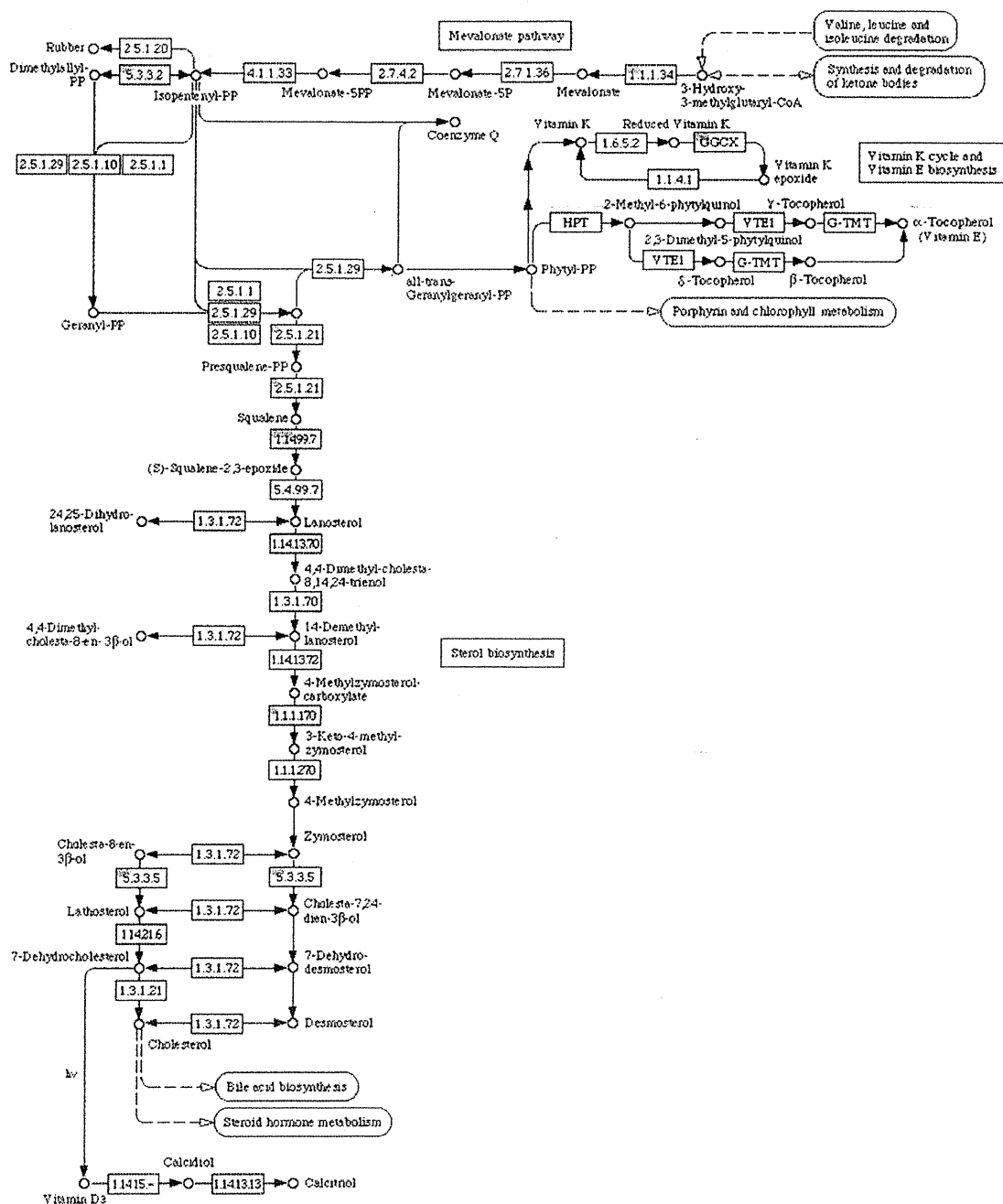


Fig. 5 KEGG Pathway map and array data (biosynthesis of steroids). Gene expression changes were mapped on the pathways. Each circle within a box represents the corresponding probe set on Human Genome U133 Plus 2.0 array because multiple probe sets are sometimes designed for a single gene. Red circles indicate overexpressed genes in cured cells compared to parental Huh7 cells. The

dotted numerical code in each box represents the Enzyme Commission (EC) number based on the recommendations of the Nomenclature Committee of the International Union of Biochemistry and Molecular Biology (IUBMB). Correspondence between the genes that were examined in the microarray analyses and enzymes that are presented in Fig. 5 is shown in Supplementary Table 4

Rep-Feo cells showed that the replication of the HCV replicon was suppressed by clofibrate and fenofibrate in a dose-dependent manner, whereas pioglitazone and troglitazone elevated expression levels of replicon. The MTS

assay did not show any effect on cell viability or replication. These results suggest that the decrease or increase in HCV replication is due to specific effects of PPAR-alpha or gamma agonists on HCV replication.

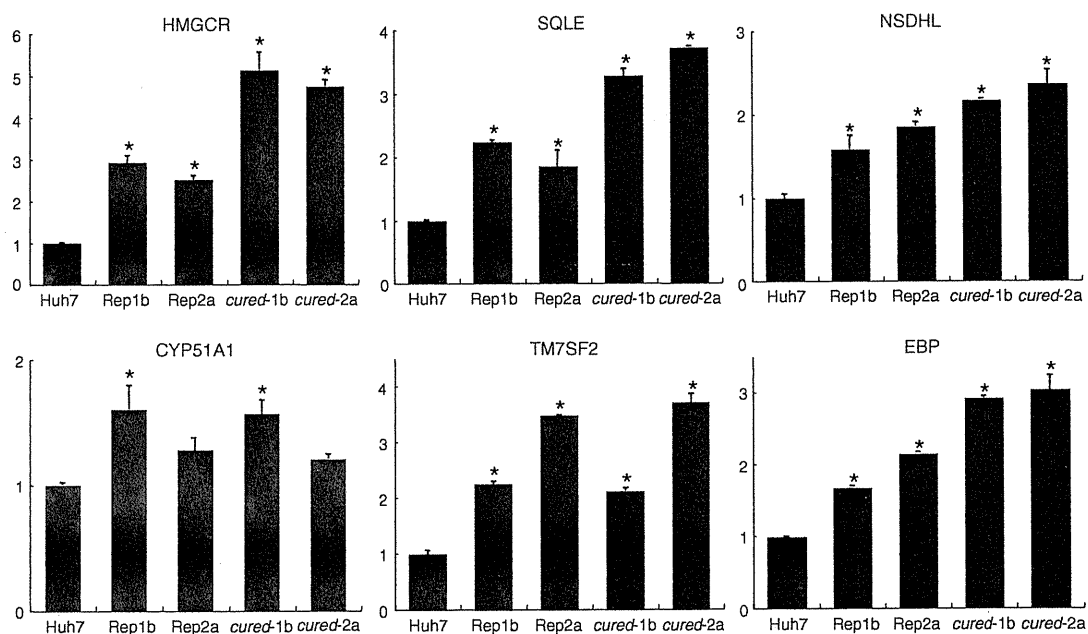


Fig. 6 Real-time detection RT-PCR. Real-time RT-PCR was performed to verify expression levels of genes that were listed in the cholesterol biosynthesis pathway in Fig. 4c and that showed

differences in their expression levels by microarray analyses. Assays were done in triplicate, and asterisks indicate *P*-values of less than 0.05

Discussion

In our present analyses, we identified MAPK signaling, biosynthesis of steroid related and TGF-beta signaling pathways as significantly changed pathway processes by comparing replicon-expressing and *cured* cells (Supplementary Table 2). The results suggest that these pathways were primarily affected by HCV replication. Comparison of *cured* cells and naïve Huh7 cells identified cell cycle, TGF-beta, sphingolipid metabolism, and biosynthesis of steroids pathways as significantly changed pathways. Interestingly, cholesterol biosynthesis pathways were significantly changed in both comparisons (Supplementary Tables 2, 3). These data suggest that these pathways may positively regulate cellular HCV replication and that cholesterol biosynthesis pathways are primarily activated by HCV replication and may be essential for continuous virus replication.

There are several studies that report gene expression changes in replicon-expressing Huh7 cells as compared with the naïve cells [30–32]. In those studies, however, the changes in gene expression do not only reflect the effect of intracellular HCV replication, but also reflect alteration of host cell clonalities. Indeed, there are inconsistencies among studies. Use of the *cured* Huh7 cells can minimize the effect of cellular clonal changes because such Huh7 subclones have already been selected through HCV replicon transduction, drug-resistance selection and subsequent HCV elimination [33]. In our study, we have compared

gene expression between genotype 1b and 2a replicon cells, respective *cured* cells and the naïve parental cells, and have identified molecular signaling or metabolic pathways that were differentially up- or down-regulated over different HCV genotypes.

Comprehensive microarray analyses and pathway analyses were very useful for the identification of molecular mechanisms of HCV infection and replication in the host cells. We used the KEGG Pathway database [28], a knowledge-based database of biological systems that integrates genomic, chemical and systemic functional information. KEGG provides a reference knowledge base for linking genome to life through the process of PATHWAY mapping, which is to map, for example, a genomic or transcriptomic content of genes to KEGG reference pathways to infer systemic behavior of the cells or the organism. These pathway databases are free on-line resources. Using these analyses, the close relation between cholesterol metabolism and HCV replication was demonstrated. Moreover, in relation to this, when we examined the pathways of other lipid metabolism, it was shown that fatty acid biosynthesis metabolism-related pathways were significantly changed in *cured* cells, and indeed we found a large number of lipid droplets in the cytosol of replicon cells and *cured* cells.

The HCV-JFH1 strain is the basis of a robustly replicating cell culture system reported recently [5]. We have performed comprehensive gene expression analyses using the HCV-JFH1 and the *cured* Huh7.5.1 cell line [6]. The

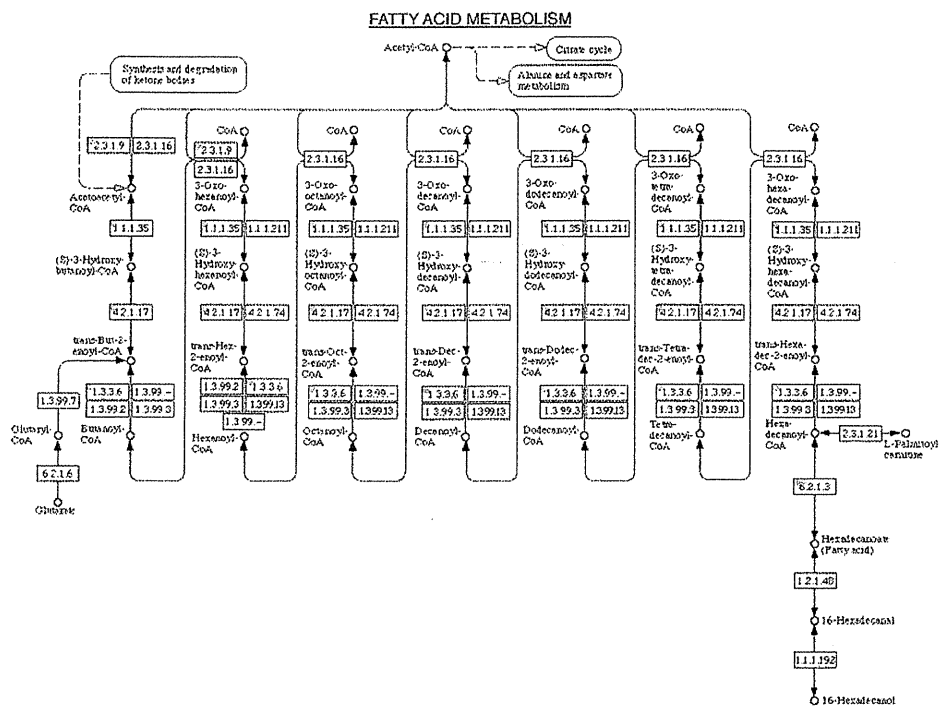
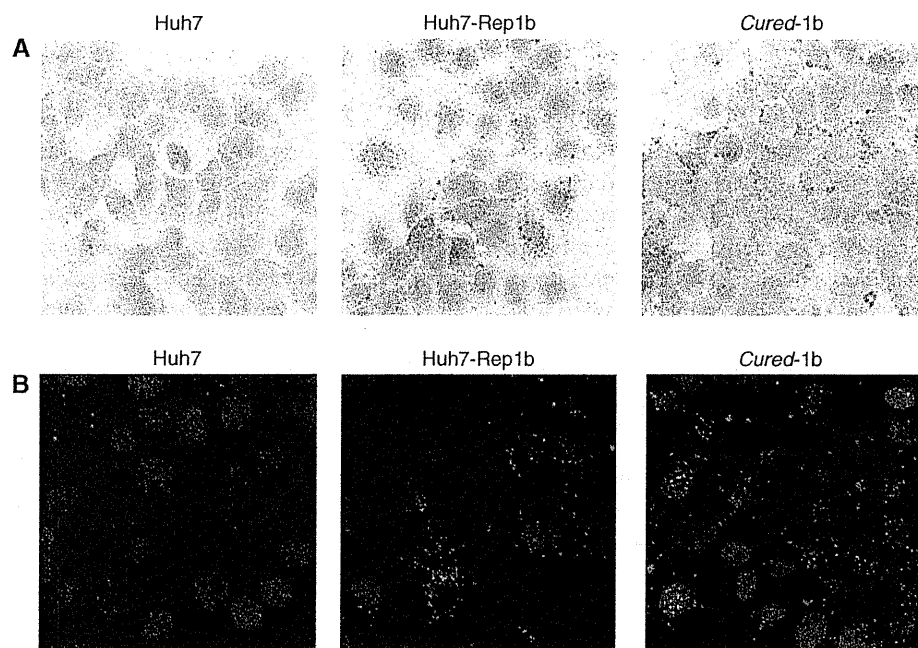


Fig. 7 KEGG Pathway map and array data (fatty acid metabolism). Gene expression changes were mapped on the pathways. Each circle within a box represents the corresponding probe set on Human Genome U133 Plus 2.0 array because multiple probe sets are sometimes designed for a single gene. Red circles indicate overexpressed genes in

cured cells compared to parental Huh7 cells. The dotted numerical code in each box represents the Enzyme Commission (EC) number. Correspondence between the genes that were examined in the microarray analyses and enzymes that are presented in Fig. 7 are shown in Supplementary Table 4

Fig. 8 Detection of intracellular lipid droplets and HCV NS protein. **a** Huh7 cells, replicon cells and cured cells were fixed and stained with Oil red O and Mayer's hematoxylin. Intracellular lipid droplets were detected as red spheres in the cells. Nuclei are stained in blue. **b** Rep1b/Huh7 cells were labeled with antibodies against NS5A (red). Lipid droplets and nuclei were stained with BODIPY493/503 (green) and DAPI (blue), respectively



KEGG Pathway analyses have identified several significantly affected pathways that are involved in the cell cycle, TGF-beta signaling, PPAR signaling and sterol

biosynthesis. These findings are consistent with our present results using the HCV subgenomic replicon (see the Supplementary Table 5; Supplementary Figs. 4, 5).

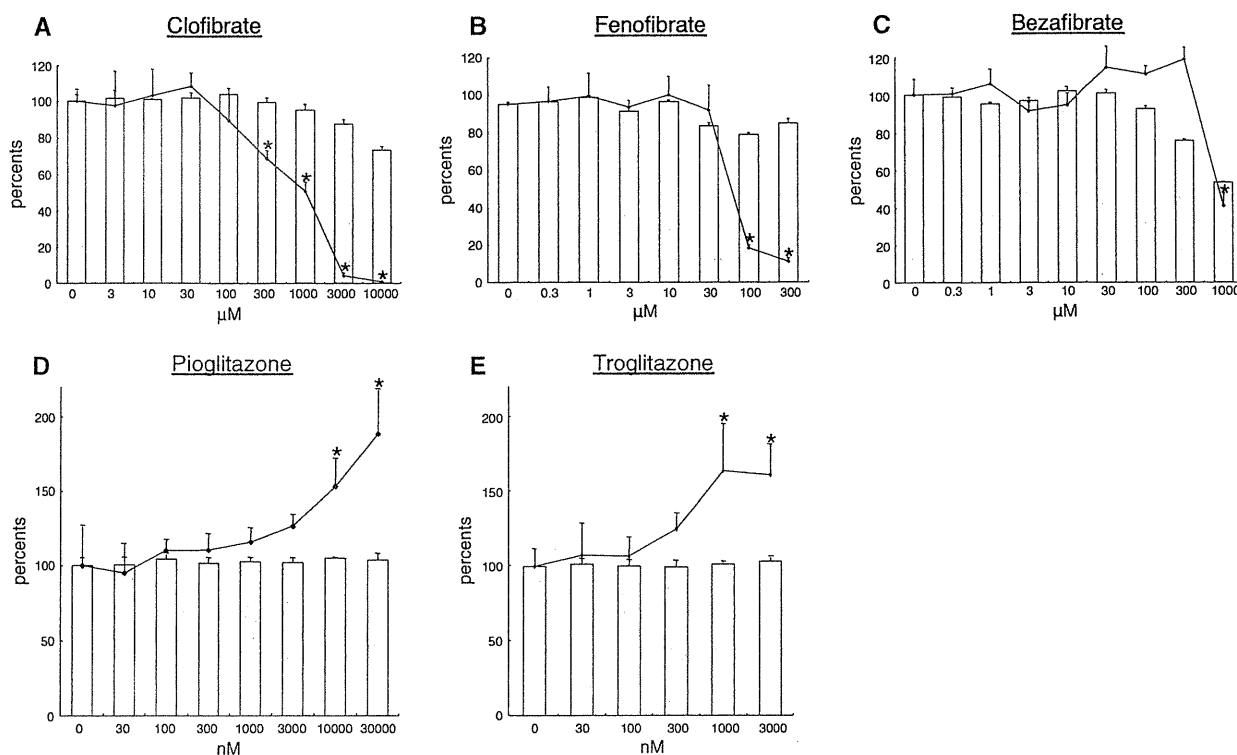


Fig. 9 Results of secondary screening with PPAR- α and - γ agonists. Luciferase activity for HCV replication levels is shown as a percentage of the control. Cell viability is also shown as percentage of

the control. Each bar represents the average of quadruplicate data points with standard deviation represented as the error bar. Asterisks denotes a significant difference from the control of at least $P < 0.05$

The JFH1 strain, however, showed substantial cytopathic effects on cultures of more than 5 days accompanied by overall induction of apoptosis-related genes and massive cell death [34]. Thus, it was difficult to conduct gene expression studies consistently.

Lipid metabolism is involved in the life cycle of many viruses. Recent studies have demonstrated the localization of HCV nonstructural proteins in the lipid raft in the endoplasmic reticulum (ER) forming intracellular replication complexes, called membranous webs [35, 36]. Because the lipid raft is enriched in cholesterol and sphingolipids, depletion of these lipids leads to inhibition of HCV genomic replication [19]. Amemiya et al. [37] reported that another serine palmitoyltransferase, myriocin, depleted cellular sphingomyelin contents and inhibited HCV replication.

It has been reported that statins efficiently suppress HCV replication in vitro and in vivo [38–40]. Statins are inhibitors of HMG-CoA reductase and shut down cholesterol biosynthesis by preventing the formation of mevalonate from 3-hydroxy-3-methyl-glutaryl CoA. As we have shown in the results, all enzymes in the cholesterol synthesis pathway were upregulated in the replicon-expressing and the cured Huh7 cells. In addition to lowering intracellular levels of sterols, statins also reduce levels of isoprenoids, which are derived from mevalonate. Isoprenoids

such as farnesyl pyrophosphate and geranylgeranyl pyrophosphate serve as lipid attachments for a variety of intracellular signaling molecules. In our results, the cholesterol biosynthesis pathway was also upregulated between cured versus naïve cell lines as well as replicon versus cured cell lines. These results suggest that HCV replication may promote synthesis of lipids including sterols that were essential for the viral efficient replication.

It has been recognized that HCV infection causes hepatic steatosis and subclinical insulin resistance and that they are independent of other risk factors such as obesity or the presence of diabetes mellitus. Similarly, in HCV cell cultures, Yang et al. [41] have reported that cellular fatty acid synthase is upregulated in HCV-infected Huh7 cells and specific inhibition of the enzymatic activity caused suppression of HCV replication. In the present study, although lipid metabolism-related genes were upregulated in cured cells, which supports efficient HCV replication, there was not significant change in lipid-related genes between replicon-expressing as compared with cured cells (Fig. 7). These results suggest that HCV subgenomic replication does not cause steatosis as it did in full-length HCV cell culture [41]. These discrepancies might be due to the absence of the presence of HCV structural genes including core and envelope proteins.

We have shown an increase in lipid droplets in HCV replicon-positive cells and their cured cell lines as a phenotype of the gene expression profiles (Fig. 8). On the other hand, ACOX1, a rate-limiting enzyme of peroxisomal beta-oxidation, was higher in cured cells than parental Huh7 cells (Fig. 7) [42]. We have shown preliminarily that cellular SREBP1 (sterol regulatory element-binding protein 1), which regulates a set of triglyceride synthesis enzymes en bloc, is upregulated in HCV replicon-positive cell lines. These discrepancies might be due to more proficient activation of SREBP1-induced fatty acid biosynthesis pathways. Collectively, our results suggest that the overall fatty acid synthesis pathway, not only fatty acid synthase, is activated by upregulation of a set of responsible enzymes.

We have investigated effects of PPAR agonists to HCV replication. PPAR-alpha agonists, clofibrate and fenofibrate suppressed HCV replication (Fig. 9). PPAR-alpha, not PPAR-gamma, is expressed in hepatocytes, recognizes cellular free fatty acids and leukotriene B4 as a specific ligands, and mediates oxidative degradation of triglyceride and depletion of intracellular fat droplets [43, 44]. These properties of PPAR-alpha agonists suggest that the level of HCV replication is affected by the increased production of fatty acids, but not by the overexpression of their related enzymes. PPAR-gamma agonists, in contrast, amplified HCV replication. Because PPAR-gamma is a regulator of fatty acid metabolism in peripheral tissue and is not expressed in the hepatocytes or in Huh7 cells (data not shown), it is possible that the effects of the PPAR-gamma agonists on HCV replication may be through its pleiotropic side effects such as p38 MAPK activation [45]. Very recently, it has been reported that HCV-NS5A proteins induce expression of PPARgamma [46].

In conclusion, comprehensive gene expression and pathway analyses were useful to study molecular pathways that were involved in HCV pathogenesis and to identify host factors for HCV replication that could constitute antiviral targets.

Acknowledgment This study was supported by grants from Ministry of Education, Culture, Sports, Science and Technology-Japan, the Japan Society for the Promotion of Science, Ministry of Health, Labour and Welfare-Japan, Japan Health Sciences Foundation, and National Institute of Biomedical Innovation.

References

- Alter MJ. Epidemiology of hepatitis C. *Hepatology*. 1997;26:62S–5S.
- Hadziyannis SJ, Sette H Jr, Morgan TR, Balan V, Diago M, Marcocellin P, et al. Peginterferon-alpha2a and ribavirin combination therapy in chronic hepatitis C: a randomized study of treatment duration and ribavirin dose. *Ann Intern Med*. 2004;140:346–55.
- Sakamoto N, Watanabe M. New therapeutic approaches to hepatitis C virus. *J Gastroenterol*. 2009;44:643–9.
- Lohmann V, Korner F, Koch J, Herian U, Theilmann L, Bartenschlager R. Replication of subgenomic hepatitis C virus RNAs in a hepatoma cell line. *Science*. 1999;285:110–3.
- Wakita T, Pietschmann T, Kato T, Date T, Miyamoto M, Zhao Z, et al. Production of infectious hepatitis C virus in tissue culture from a cloned viral genome. *Nat Med*. 2005;11:791–6.
- Zhong J, Gastaminza P, Cheng G, Kapadia S, Kato T, Burton DR, et al. Robust hepatitis C virus infection in vitro. *Proc Natl Acad Sci USA*. 2005;102:9294–9.
- Tai AW, Benita Y, Peng LF, Kim SS, Sakamoto N, Xavier RJ, et al. A functional genomic screen identifies cellular cofactors of hepatitis C virus replication. *Cell Host Microbe*. 2009;5:298–307.
- Itsui Y, Sakamoto N, Kurosaki M, Kanazawa N, Tanabe Y, Koyama T, et al. Expression screening of interferon-stimulated genes for antiviral activity against hepatitis C virus replication. *J Viral Hepat*. 2006;13:690–700.
- Yamashiro T, Sakamoto N, Kurosaki M, Kanazawa N, Tanabe Y, Nakagawa M, et al. Negative regulation of intracellular hepatitis C virus replication by interferon regulatory factor 3. *J Gastroenterol*. 2006;41:750–7.
- Foy E, Li K, Sumpter R Jr, Loo YM, Johnson CL, Wang C, et al. Control of antiviral defenses through hepatitis C virus disruption of retinoic acid-inducible gene-I signaling. *Proc Natl Acad Sci USA*. 2005;102:2986–91.
- Sakamoto N, Yoshimura M, Kimura T, Toyama K, Sekine-Osajima Y, Watanabe M, et al. Bone morphogenetic protein-7 and interferon-alpha synergistically suppress hepatitis C virus replication. *Biochem Biophys Res Commun*. 2007;357:467–73.
- Murata T, Ohshima T, Yamaji M, Hosaka M, Miyanari Y, Hijikata M, et al. Suppression of hepatitis C virus replication by TGF-beta. *Virology*. 2005;331:407–17.
- Shimakami T, Honda M, Kusakawa T, Murata T, Shimotohno K, Kaneko S, et al. Effect of hepatitis C virus (HCV) NS5B-nucleolin interaction on HCV replication with HCV subgenomic replicon. *J Virol*. 2006;80:3332–40.
- Nakagawa M, Sakamoto N, Tanabe Y, Koyama T, Itsui Y, Takeda Y, et al. Suppression of hepatitis C virus replication by cyclosporin a is mediated by blockade of cyclophilins. *Gastroenterology*. 2005;129:1031–41.
- Tardif KD, Mori K, Siddiqui A. Hepatitis C virus subgenomic replicons induce endoplasmic reticulum stress activating an intracellular signaling pathway. *J Virol*. 2002;76:7453–9.
- Wang J, Tong W, Zhang X, Chen L, Yi Z, Pan T, et al. Hepatitis C virus non-structural protein NS5A interacts with FKBP38 and inhibits apoptosis in Huh7 hepatoma cells. *FEBS Lett*. 2006;580:4392–400.
- Choi YW, Tan YJ, Lim SG, Hong W, Goh PY. Proteomic approach identifies HSP27 as an interacting partner of the hepatitis C virus NS5A protein. *Biochem Biophys Res Commun*. 2004;318:514–9.
- Okamoto T, Nishimura Y, Ichimura T, Suzuki K, Miyamura T, Suzuki T, et al. Hepatitis C virus RNA replication is regulated by FKBP8 and Hsp90. *EMBO J*. 2006;25:5015–25.
- Sakamoto H, Okamoto K, Aoki M, Kato H, Katsume A, Ohta A, et al. Host sphingolipid biosynthesis as a target for hepatitis C virus therapy. *Nat Chem Biol*. 2005;1:333–7.
- Yokota T, Sakamoto N, Enomoto N, Tanabe Y, Miyagishi M, Maekawa S, et al. Inhibition of intracellular hepatitis C virus replication by synthetic and vector-derived small interfering RNAs. *EMBO Rep*. 2003;4:602–8.
- Tanabe Y, Sakamoto N, Enomoto N, Kurosaki M, Ueda E, Maekawa S, et al. Synergistic inhibition of intracellular hepatitis C virus replication by combination of ribavirin and interferon-alpha. *J Infect Dis*. 2004;189:1129–39.

22. Guo JT, Bichko VV, Seeger C. Effect of alpha interferon on the hepatitis C virus replicon. *J Virol*. 2001;75:8516–23.
23. Donnelly MLL, Hughes LE, Luke G, Mendoza H, ten Dam E, Gani D, et al. The 'cleavage' activities of foot-and-mouth disease virus 2A site-directed mutants and naturally occurring '2A-like' sequences. *J Gen Virol*. 2001;82:1027–41.
24. Nakagawa M, Sakamoto N, Enomoto N, Tanabe Y, Kanazawa N, Koyama T, et al. Specific inhibition of hepatitis C virus replication by cyclosporin A. *Biochem Biophys Res Commun*. 2004;313:42–7.
25. Blight KJ, McKeating JA, Rice CM. Highly permissive cell lines for subgenomic and genomic hepatitis C virus RNA replication. *J Virol*. 2002;76:13001–14.
26. Strand C, Enell J, Hedenfalk I, Ferno M. RNA quality in frozen breast cancer samples and the influence on gene expression analysis—a comparison of three evaluation methods using microcapillary electrophoresis traces. *BMC Mol Biol*. 2007;8:38.
27. Tusher VG, Tibshirani R, Chu G. Significance analysis of microarrays applied to the ionizing radiation response. *Proc Natl Acad Sci USA*. 2001;98:5116–21.
28. Kanehisa M, Araki M, Goto S, Hattori M, Hirakawa M, Itoh M, et al. KEGG for linking genomes to life and the environment. *Nucleic Acids Res*. 2008;36:D480–4.
29. Benjamini Y, Hochberg Y. Controlling the false discovery rate: a practical and powerful approach to multiple testing. *J R Stat Soc B*. 1995;57:289–300.
30. Ciccaglione AR, Marcantonio C, Tritarelli E, Tataseo P, Ferraris A, Bruni R, et al. Microarray analysis identifies a common set of cellular genes modulated by different HCV replicon clones. *BMC Genomics*. 2008;9:309.
31. Hayashi J, Stoyanova R, Seeger C. The transcriptome of HCV replicon expressing cell lines in the presence of alpha interferon. *Virology*. 2005;335:264–75.
32. Scholle F, Li K, Bodola F, Ikeda M, Luxon BA, Lemon SM. Virus–host cell interactions during hepatitis C virus RNA replication: impact of polyprotein expression on the cellular transcriptome and cell cycle association with viral RNA synthesis. *J Virol*. 2004;78:1513–24.
33. Abe K, Ikeda M, Dansako H, Naka K, Shimotohno K, Kato N. cDNA microarray analysis to compare HCV subgenomic replicon cells with their cured cells. *Virus Res*. 2005;107:73–81.
34. Sekine-Osajima Y, Sakamoto N, Nakagawa M, Itsui Y, Tasaka M, Nishimura-Sakurai Y, et al. Development of plaque assays for hepatitis C virus and isolation of mutants with enhanced cytopathogenicity and replication capacity. *Virology*. 2008;371:71–85.
35. Mottola G, Cardinali G, Ceccacci A, Trozzi C, Bartholomew L, Torrisi MR, et al. Hepatitis C virus nonstructural proteins are localized in a modified endoplasmic reticulum of cells expressing viral subgenomic replicons. *Virology*. 2002;293:31–43.
36. Gosert R, Egger D, Lohmann V, Bartenschlager R, Blum HE, Bienz K, et al. Identification of the hepatitis C virus RNA replication complex in Huh-7 cells harboring subgenomic replicons. *J Virol*. 2003;77:5487–92.
37. Amemiya F, Maekawa S, Itakura Y, Kanayama A, Takano S, Yamaguchi T, et al. Targeting lipid metabolism in the treatment of hepatitis C. *J Infect Dis*. 2008;197:361–70.
38. Ikeda M, Abe K, Yamada M, Dansako H, Naka K, Kato N. Different anti-HCV profiles of statins and their potential for combination therapy with interferon. *Hepatology*. 2006;44:117–25.
39. Kim SS, Peng LF, Lin W, Choe WH, Sakamoto N, Kato N, et al. A cell-based, high-throughput screen for small molecule regulators of hepatitis C virus replication. *Gastroenterology*. 2007;132:311–20.
40. Bader T, Fazili J, Madhoun M, Aston C, Hughes D, Rizvi S, et al. Fluvastatin inhibits hepatitis C replication in humans. *Am J Gastroenterol*. 2008;103:1383–9.
41. Yang W, Hood BL, Chadwick SL, Liu S, Watkins SC, Luo G, et al. Fatty acid synthase is up-regulated during hepatitis C virus infection and regulates hepatitis C virus entry and production. *Hepatology*. 2008;48:1396–403.
42. Li Y, Tharappel JC, Gooper S, Glenn M, Glauert HP, Spear BT. Expression of the hydrogen peroxide-generating enzyme fatty acyl CoA oxidase activates NF-kappaB. *DNA Cell Biol*. 2000;19:113–20.
43. Costet P, Legendre C, More J, Edgar A, Galtier P, Pineau T. Peroxisome proliferator-activated receptor alpha-isoform deficiency leads to progressive dyslipidemia with sexually dimorphic obesity and steatosis. *J Biol Chem*. 1998;273:29577–85.
44. Kersten S, Seydoux J, Peters JM, Gonzalez FJ, Desvergne B, Wahli W. Peroxisome proliferator-activated receptor alpha mediates the adaptive response to fasting. *J Clin Invest*. 1999;103:1489–98.
45. Schiefelbein D, Seitz O, Goren I, Dissmann JP, Schmidt H, Bachmann M, et al. Keratinocyte-derived vascular endothelial growth factor biosynthesis represents a pleiotropic side effect of peroxisome proliferator-activated receptor-gamma agonist troglitazone but not rosiglitazone and involves activation of p38 mitogen-activated protein kinase: implications for diabetes-impaired skin repair. *Mol Pharmacol*. 2008;74:952–63.
46. Kim K, Kim KH, Ha E, Park JY, Sakamoto N, Cheong J. Hepatitis C virus NS5A protein increases hepatic lipid accumulation via induction of activation and expression of PPARgamma. *FEBS Lett*. 2009;583:2720–6.
47. Kato T, Date T, Miyamoto M, Furusaka A, Tokushige K, Mizokami M, et al. Efficient replication of the genotype 2a hepatitis C virus subgenomic replicon. *Gastroenterology*. 2003;125:1808–17.

Mutations in the interferon sensitivity determining region and virological response to combination therapy with pegylated-interferon alpha 2b plus ribavirin in patients with chronic hepatitis C-1b infection

Mina Nakagawa · Naoya Sakamoto · Mayumi Ueyama · Kaoru Mogushi · Satoshi Nagaie · Yasuhiro Itsui · Seishin Azuma · Sei Kakinuma · Hiroshi Tanaka · Nobuyuki Enomoto · Mamoru Watanabe

Received: 1 June 2009 / Accepted: 11 December 2009
© Springer 2010

Abstract

Background Pegylated-interferon-alpha 2b (PEG-IFN) plus ribavirin (RBV) therapy is currently the de-facto standard treatment for hepatitis C virus (HCV) infection. The aims of this study were to analyze the clinical and virological factors associated with a higher rate of response in patients with HCV genotype 1b infection treated with combination therapy.

Methods We analyzed, retrospectively, 239 patients with chronic hepatitis C-1b infection who received 48 weeks of combination therapy. We assessed clinical and laboratory parameters, including age, gender, pretreatment hemoglobin, platelet counts, HCV RNA titer, liver histology, the

number of interferon sensitivity determining region (ISDR) mutations and substitutions of the core amino acids 70 and 91. Drug adherence was monitored in each patient. We carried out univariate and multivariate statistical analyses of these parameters and clinical responses.

Results On an intention-to-treat (ITT) analysis, 98 of the 239 patients (41%) had sustained virological responses (SVRs). Patients with more than two mutations in the ISDR had significantly higher SVR rates ($P < 0.01$). Univariate analyses showed that stage of fibrosis, hemoglobin, platelet counts, ISDR mutations, serum HCV RNA level, and adherence to PEG-IFN plus RBV were significantly correlated with SVR rates. Multivariate analysis in subjects with good drug adherence extracted the number of ISDR mutations (two or more: odds ratio [OR] 5.181).

Conclusions The number of mutations in the ISDR sequence of HCV-1b (≥ 2) is the most effective parameter predicting a favorable clinical outcome of 48-week PEG-IFN plus RBV therapy in patients with HCV genotype 1b infection.

M. Nakagawa and N. Sakamoto contributed equally to this work.

M. Nakagawa · N. Sakamoto (✉) · M. Ueyama · Y. Itsui · S. Azuma · S. Kakinuma · M. Watanabe
Department of Gastroenterology and Hepatology,
Tokyo Medical and Dental University, 1-5-45 Yushima,
Bunkyo-ku, Tokyo 113-8519, Japan
e-mail: nsakamoto.gast@tmd.ac.jp

M. Nakagawa · N. Sakamoto · S. Kakinuma
Department for Hepatitis Control,
Tokyo Medical and Dental University, Tokyo, Japan

K. Mogushi · S. Nagaie · H. Tanaka
Information Center for Medical Science,
Tokyo Medical and Dental University, Tokyo, Japan

Y. Itsui
Department of Internal Medicine,
Soka Municipal Hospital, Saitama, Japan

N. Enomoto
First Department of Internal Medicine,
University of Yamanashi, Yamanashi, Japan

Keywords Hepatitis C virus (HCV) · Chronic hepatitis C · PEG-IFN plus RBV therapy · Combination therapy · Interferon sensitivity determining region (ISDR)

Abbreviations

HCV	Hepatitis C virus
IFN	Interferon
PEG	Polyethylene glycol
PEG-IFN	Pegylated-interferon-alpha 2b
RBV	Ribavirin
ISDR	Interferon sensitivity determining region
BMI	Body mass index

ALT	Alanine transaminase
dM	Double mutant
ITT analysis	Intention-to-treat analysis
PP analysis	Per protocol analysis
SVR	Sustained virological response
ETR	End of treatment response
PKR	Double stranded RNA-dependent protein kinase
TLR	Toll-like receptor
MyD88	Myeloid differentiation primary response gene 88

Introduction

Hepatitis C virus (HCV) is one of the major pathogens causing chronic hepatitis [1, 2] and eradication of the virus by the host occurs infrequently during the natural course of infection once it becomes chronic. Interferon (IFN) has been used widely as the most effective antiviral agent for chronic hepatitis C. Although ribavirin (RBV), a synthetic guanosine analog, alone does not decrease the serum HCV RNA level [3–5], it has been shown that combination therapy with IFN- α (given 3 times weekly) and daily RBV gives a higher sustained response rate than IFN monotherapy [6–8]. Pegylation is the process by which an inert molecule of polyethylene glycol (PEG) is covalently attached to a protein, and the addition of PEG to IFN produces a biologically active molecule with a longer half-life and more favorable pharmacokinetics than the natural molecule. These characteristics allow more convenient, once-weekly dosing [9]. Pegylated (PEG)-IFN plus RBV is significantly more effective than IFN plus RBV or PEG-IFN alone for the treatment of chronic hepatitis C, with sustained virological response rates of ~50% in patients infected with HCV genotype 1b [10].

We reported previously a close correlation between the number of mutations in the nonstructural 5A (NS5A) region of the HCV genome encoding amino acids (aa) at positions 2209–2248 [the IFN sensitivity determining region (ISDR)] and IFN efficacy in patients with HCV genotype 1b infection [11–13]. The aims of this study were to analyze clinical and virological factors associated with a higher rate of response by patients with HCV genotype 1b infection who were treated with combination therapy with pegylated-IFN- α 2b (PEG-IFN) plus RBV, and to clarify the relationship between ISDR mutations and virological response to the combination therapy.

Methods

Patients and methods

We analyzed, retrospectively, 239 patients with chronic HCV-1b infection who received combination therapy with PEG-IFN plus RBV between December 2004 and April 2008 at Tokyo Medical and Dental University Hospital (Tokyo, Japan) and associated hospitals participating in the Ochanomizu-Liver Conference Study Group. All patients had histologically or clinically proven chronic active hepatitis and were positive for anti-HCV antibodies and serum HCV RNA by reverse transcription polymerase chain reaction (RT-PCR). Patients with a positive test for serum hepatitis B surface antigen, coinfection with other HCV genotypes, coinfection with human immunodeficiency virus, other causes of hepatocellular injury (such as alcoholism, autoimmune hepatitis, primary biliary cirrhosis, or a history of treatment with hepatotoxic drugs), and a need for hemodialysis were excluded.

The following factors were analyzed to determine whether they were related to the efficacy of combination therapy: age; gender; body mass index (BMI); previous IFN therapy; grade of inflammation and stage of fibrosis on liver biopsy; pretreatment biochemical parameters, such as hemoglobin, alanine transaminase (ALT) level, platelet count, low density lipoprotein (LDL) cholesterol, serum HCV RNA level (Log IU/ml); and the amino acid sequence of the IFN sensitivity determining region (aa 2209–2248, ISDR). Liver biopsy specimens were evaluated according to the grade of inflammation and the stage of fibrosis; this was done blindly by an independent interpreter who was not aware of the clinical data. Activity of inflammation was graded on a scale of 0–3: A0 shows no activity, A1 shows mild activity, A2 shows moderate activity, and A3 shows severe activity. Fibrosis was staged on a scale of 0–4: F0 shows no fibrosis, F1 shows moderate fibrosis, F2 shows moderate fibrosis with few septa, F3 shows severe fibrosis with numerous septa without cirrhosis, and F4 shows cirrhosis.

The study protocol conformed to the ethical guidelines of the Declaration of Helsinki and was approved by the ethics committee of our hospital, and informed written consent was obtained from each patient.

Nucleotide sequencing of the NS5A gene

The serum samples were frozen at -80°C until use. Extraction of RNA from serum and RT-PCR were performed as described previously [14]. The PCR and sequencing primers were synthesized with a DNA synthesizer (model 391; Applied Biosystems Japan, Chiba, Japan).